UNIVERSITY OF ILLINOIS
URBANA

AERONOMY REPORT NO. 47

DIFFERENTIAL PHASE MEASUREMENTS OF D-REGION PARTIAL REFLECTIONS

by

D. J. Wiersma
C. F. Sechrist, Jr.

March 1, 1972

Supported by
National Aeronautics and Space Administration
Grant NGR 14-005-181

Aeronomy Laboratory
Department of Electrical Engineering
University of Illinois
Urbana, Illinois

CITATION POLICY

The material contained in this report is preliminary information circulated rapidly in the interest of prompt interchange of scientific information and may be later revised on publication in accepted aeronomic journals. It would therefore be appreciated if persons wishing to cite work contained herein would first contact the authors to ascertain if the relevant material is part of a paper published or in process.

UILU-Eng 72 2502

A E R O N O M Y R E P O R T

N O. 47

DIFFERENTIAL PHASE MEASUREMENTS OF D-REGION PARTIAL REFLECTIONS

by

D. J. Wiersma
C. F. Sechrist, Jr.

March 1, 1972

Supported by
National Aeronautics and
Space Administration
Grant NGR 14-005-181

Aeronomy Laboratory
Department of Electrical Engineering
University of Illinois
Urbana, Illinois

ABSTRACT

Differential-phase partial-reflection measurements have been used to deduce D-region electron-density profiles. The phase difference was measured by taking sums and differences of amplitudes received on an array of crossed dipoles. The reflection model used was derived from Fresnel reflection theory. Seven profiles obtained over the period from October 13, 1971 to November 5, 1971, are presented along with the results from simultaneous measurements of differential absorption. Some possible sources of error as well as error propagation are discussed. A collision-frequency profile is deduced from the electron concentration calculated from differential phase and differential absorption. It is concluded that the differential phase measurement would be a useful addition to the partial-reflection experiment.

TABLE OF CONTENTS

Page

ABSTRACT iii

LIST OF FIGURES v

LIST OF TABLES vii

1. INTRODUCTION 1

2. RADIO WAVES IN THE IONOSPHERE 4

3. THE THEORY OF PARTIAL REFLECTIONS 11

3.1 Fresnel Reflection Theory 11
3.2 Volume Scattering Thoery 15

4. DIFFERENTIAL PHASE MEASURING SYSTEM 21

4.1 Angle of Phase Difference 21
4.2 Differential Phase Measuring System 27

5. RESULTS OF DIFFERENTIAL PHASE MEASUREMENTS 37

6. DIFFERENTIAL PHASE SYSTEM EVALUATION 49

6.1 Uncertainties in Measurement Techniques 49
6.2 Assumptions and Theories 53
6.3 Collision Frequency 56

7. CONCLUSIONS AND SUGGESTIONS FOR FURTHER WORK 59

REFERENCES 61

APPENDIX 63

LIST OF FIGURES

Figure		Page
3.1	Electron concentration profiles from rocket measurements (after Mechtly and Smith, 1968)	16
3.2	Difference between phase components of the reflection coefficients calculated from rocket measurements	17
3.3	Phase difference versus altitude calculated from electron concentration profiles measured by rockets	18
4.1	Block diagram of differential phase partial reflection system	28
4.2	Differential phase transmitter antenna polarization network	30
4.3	Differential phase receiver antenna polarization network	32
4.4	Antenna polarizations required to obtain the amplitudes A_o, A_x, A_1, A_2, A_3, and A_4	33
5.1	Collision frequency profile used for calculating electron concentrations from both differential phase and differential absorption	38
5.2	Phase difference amplitude ratio, and amplitude of the correlation coefficient versus altitude	39
5.3	Phase difference amplitude ratio, and amplitude of the correlation coefficient versus altitude	40
5.4	Electron concentration versus altitude from differential phase and differential absorption (October 13, 1971) $\chi = 56°$	42
5.5	Electron concentration versus altitude from differential phase and differential absorption (October 14, 1971) $\chi = 52°$	43
5.6	Electron concentration versus altitude from differential phase and differential absorption (October 19, 1971) $\chi = 55°$	44

Figure | Page

5.7 Electron concentration versus altitude from differential phase and differential absorption (October 19, 1971) $\chi = 54°$ 45

5.8 Electron concentration versus altitude from differential phase and differential absorption (October 28, 1971) $\chi = 53°$ 46

5.9 Electron concentration versus altitude from differential phase and differential absorption (October 28, 1971) $\chi = 56°$ P.M. 47

5.10 Electron concentration versus altitude from differential phase and differential absorption (November 4, 1971) $\chi = 55°$ 48

6.1 Collision frequency profile deduced from differential phase and differential absorption measurements. 58

1. INTRODUCTION

The D region (50-90 kilometers) is probably the most complex and least understood region in the ionosphere. Efforts to describe the D-region have been hampered by the complexity of the neutral and ion chemistry and the difficulties associated with measurements at these altitides. The parameters of the lower ionosphere which can be used to understand the processes that occur must be measured accurately and reliably. One parameter, which is important in the ionosphere and particularly in the D region, is the electron concentration. One goal of an experimental aeronomer, then, is to develop a system which can measure the electron concentration with sufficient accuracy that a reasonable description of the ionosphere can be made.

Measurements of electron concentration can be made by sounding rockets or by ground-based techniques. Rocket measurements of D-region electron concentrations and collision frequencies have become quite sophisticated and are believed to be accurate (Mechtly, et al. 1967). However, because of cost limitations, only a limited number of rockets can be used to gather information. Also, sounding rockets can only be launched from relatively few locations. The disadvantage of ground-based experiments is that the data are more difficult to interpret. However, ground-based experiments can be set up in a variety of locations and can be operated continuously or as required. Thus, large amounts of data from several locations can be used to study diurnal, seasonal, and geographical variations.

One such ground-based technique for measuring electron concentrations in the D region is the partial-reflection experiment. Weak reflections from the D region are used to calculate the electron concentration over a range of altitudes. Gardner and Pawsey (1953) were the first to use a partial-reflection

system to obtain electron-concentration profiles. Since then several experimenters, for example, Belrose and Burke (1964), Pirnat and Bowhill (1966), Thrane, et al. (1967), Gregory and Manson (1967), and Birley and Sechrist (1971), have developed the partial-reflection experiment to the point where it provides useful quantitative measurements of the electron-density distribution in the lower ionosphere.

Most of the partial-reflection measurements that have been made are of differential absorption. Fejer (1961) suggested that the partial-reflection technique be modified to include measurements of the phase difference between the two magneto-ionic modes. Differential phase measurements would add a simultaneous independent electron concentration measurement which along with differential absorption might subsequently be used to deduce a collision-frequency profile. Belrose (1970) also suggested the measurement of differential phase to improve the partial-reflection technique.

Two methods of measuring the phase of a received signal are possible. The first method, suggested separately by Connolly (1971) and by Austin (1971), compares the phase of each magneto-ionic mode in order to obtain a voltage proportional to the difference in phases. Connolly did some calculations of expected experimental results. He concluded that differential phase measurements when combined with differential absorption would provide better electron density and collision frequency data from 70 to 90 kilometers. Austin performed a direct phase measurement and obtained one electron density which showed reasonable values for electron concentration. The experimental arrangement that he used is described by Austin, et al. (1969).

The second method which was used by von Biel, et al. (1970) and von Biel (1971) obtains the phase difference by measuring mean-squared amplitudes with

different antenna polarizations. From these amplitudes a correlation coefficient is calculated which is dependent on the integral over the propagation path of the phases of the two magneto-ionic modes. These investigators obtained reasonable results, although extensive data collection was not made.

At the University of Illinois Aeronomy Field Station a system for measuring differential phase has been set up in conjunction with the existing partial-reflection experiment. The method used is similar to that of von Biel, et al. (1970) and von Biel (1971). In Chapter 2 definitions and relations necessary to calculate electron concentrations from differential phase measurements are given. A development of the Fresnel reflection theory along with volume scattering theory is presented in Chapter 3. Also a discussion of the significance of each theory as applied to differential phase partial-reflection measurements is given. Chapter 4 describes the system used to obtain phase measurements as well as the procedure for making these measurements. Electron concentration profiles obtained by this system are presented in Chapter 5. A critical evaluation of the system is made in Chapter 6. Possible sources of error and their effects on electron concentration calculations are considered. Also, the differential phase system is evaluated as a possible tool for studying D-region ionization. In the final chapter conclusions and suggestions for further work are given. The computer programs used to process the differential phase data are listed in the appendix.

2. RADIO WAVES IN THE IONOSPHERE

An electromagnetic wave propagating through a medium can be described by the expression for the electric field intensity vector

$$\vec{E} = \vec{\mathcal{E}} \exp[j(\omega t - \vec{k} \cdot \vec{r})] \tag{2.1}$$

where ω is the operating angular frequency, $\vec{k}$ is the propagation vector in the direction of phase propagation, and $\vec{r}$ is the position vector. As the wave propagates through the medium, the magnitude and phase of $\vec{E}$ change as $\vec{k}$ and $\vec{r}$ change. These changes in $\vec{k}$ imply that the medium has an effect on the wave as it propagates. By measuring the changes in the magnitude and phase of $\vec{E}$, information about the medium such as the electron concentration can be deduced.

The medium which will be considered here is the D region of the ionosphere. Since the earth's ionosphere consists of a homogeneous admixture of neutral and ionized species immersed in the earth's magnetic field, it is termed a magneto-ionic medium. As a magneto-ionic medium, however, the ionosphere is relatively weakly ionized. The concentration of free electrons which are largely produced by photoionization is on the order of 10^7 to 10^9 m^{-3} during the day. Both the magnetic field and the ionization have a significant effect on the propagation vector $\vec{k}$.

Another important parameter of a magneto-ionic medium is the collision frequency. The number of collisions between electrons and neutral particles per second is termed the collision frequency and is represented by the symbol ν_m. Other collisions such as electron-electron, neutral-neutral, or neutral-ion do not have a significant effect on radio waves due to the mass of the particles

or the small number of collisions. A knowledge of the electron-neutral collision frequency as a function of altitude is necessary for the expressions which describe the effect of the medium on the wave. A more detailed treatment of collision frequencies and their measurement is given by Lodato and Mechtly (1971).

The propagation vector $\vec{k}$ depends on the refractive index n of the medium and is given by

$$\vec{k} = \frac{2\pi}{\lambda} n \cdot \hat{k} \tag{2.2}$$

where λ is the wavelength of the operating frequency and $\hat{k}$ is a unit vector. The refractive index is defined as the ratio of the speed of light in a vacuum c to the phase velocity of the wave v_p in the magneto-ionic medium and is given by

$$n = \frac{c}{v_p} = \sqrt{\varepsilon_r} \tag{2.3}$$

where ε_r is the relative permittivity of the medium. The relative permeability will be taken to be unity for the ionosphere.

A wave traveling in the $\hat{z}$ direction will have components of the electric field intensity vector $\vec{E}$ and the magnetic field intensity vector $\vec{H}$ in the $\hat{x}$ and $\hat{y}$ directions. The polarization of the radio wave is defined by

$$R \equiv E_y/E_x = - H_x/H_y \ . \tag{2.4}$$

When the wave polarization R is equal to a constant the wave is propagated through the medium without changing its polarization. For a magneto-ionic

medium there are two of these characteristic waves, the ordinary and the extraordinary. The absorption and phase shift of the extraordinary wave is significantly greater than for the ordinary wave. North of the magnetic equator the field vectors of the ordinary wave rotate from north into west, and the field vectors of the extraordinary wave rotate from north into east.

The effect of the magneto-ionic medium on $\vec{k}$ can be described by considering a wave traveling through the medium.

$$\vec{E} = \vec{\mathcal{E}} \exp[-j(\vec{k} \cdot \vec{r})] \tag{2.5}$$

The time dependence has been suppressed. The propagation vector in one direction (z) is given by

$$k_z = (2\pi/\lambda) \int_{\ell} n_{o,x} \, dz \tag{2.6}$$

The subscripts o and x refer to the ordinary and extraordinary waves, respectively. By substituting Equation (2.6) into (2.5), the expression for the wave can be written as

$$\vec{E}_{o,x} = \vec{\mathcal{E}} \exp[-j(\frac{2\pi}{\lambda} \int_{\ell} n_{o,x} \, dz)] \tag{2.7}$$

By separating the refractive index into its real and imaginary parts (2.7) can be written as

$$\vec{E}_{o,x} = \vec{\mathcal{E}} \exp[-\frac{2\pi}{\lambda} \int_{\ell} n^{i}_{o,x} \, dz] \cdot \exp[-j(\frac{2\pi}{\lambda} \int_{\ell} n^{r}_{o,x} \, dz)] \tag{2.8}$$

where the superscripts r and i denote the real and imaginary parts of the refractive index. As the wave travels through the medium it is absorbed and the phase is changed. The absorption depends on the integral of the imaginary part of the refractive index over the path. The change in phase is a function of the integral of the real part of the refractive index over the path that the wave travels.

The ratio of the returned electric field strength vector of the extraordinary wave to that of the ordinary wave is given by

$$\vec{E}_x/\vec{E}_o = \exp[-\frac{2\pi}{\lambda}\int_{\ell}(n_x^i - n_o^i)dz] \cdot \exp[-j\frac{2\pi}{\lambda}\int_{\ell}(n_x^r - n_o^r)dz] \ . \qquad (2.9)$$

The phase angle of this ratio can be taken from equation 2.9

$$\Delta\phi = \frac{2\pi}{\lambda}\int_{\ell}(n_o^r - n_x^r)dz \ . \qquad (2.10)$$

Alternatively the expression for $\Delta\phi$ can be described as the difference between the phase angles of the ordinary and extraordinary mode of polarization. This difference $\Delta\phi$ is the phase difference which is to be measured.

In the development of magneto-ionic theory an expression is derived for the refractive index in terms of the electron concentration, the collision frequency, the operating frequency, and the magnetic field. The classical Appleton-Hartree formulas were used by Gardner and Pawsey (1953) and other earlier experimenters. A full treatment of the Appleton-Hartree formulation is presented by Ratcliffe (1959). Sen and Wyller (1960) derived a generalized magneto-ionic theory and corresponding formula for the refractive index. The use of the

generalized formula is necessary for calculations in the D region. For mid-latitudes the quasi-longitudinal approximation can be used with negligible error. The quasi-longitudinal approximation to the complex refractive index is given by

$$n = n^{r}_{o,x} - j\, n^{i}_{o,x}$$

$$\approx \left[1 - \frac{\omega_N^2}{\omega\nu_m}\left(\frac{\omega \pm \omega_L}{\nu_m}\right) \mathcal{C}_{3/2}\left(\frac{\omega \pm \omega_L}{\nu_m}\right) - j\, 5/2\, \frac{\omega_N^2}{\omega\nu_m}\, \mathcal{C}_{5/2}\left(\frac{\omega \pm \omega_L}{\nu_m}\right)\right]^{1/2} \qquad (2.11)$$

where ω_L is the longitudinal component of the electron gyrofrequency. ω_N is the plasma frequency and is given by

$$\omega_N^2 = \frac{Ne^2}{m\varepsilon_o} \qquad s^{-2} \qquad (2.12)$$

where N is the electron concentration m^{-3}; e is the electronic charge C; m is the mass of an electron kg; and ε_o is the dielectric constant Fm^{-1}. $\mathcal{C}_p$ is the semiconductor integral. Approximate formulas for evaluating $\mathcal{C}_p$ are found in Hara (1963). The real and imaginary parts of the refractive index ($n^{r}_{o,x}$ and $n^{i}_{o,x}$) can be found by expanding (2.11) by the binomial theorem.

$$n_{o,x} = \left[1 - \frac{\omega_N^2}{\omega\nu_m}\left(\frac{\omega \pm \omega_L}{\nu_m}\right) \mathcal{C}_{3/2}\left(\frac{\omega \pm \omega_L}{\nu_m}\right)\right]^{1/2}$$

$$-j\ 1/2\left[5/2\, \frac{\omega_N^2}{\omega\nu_m}\, \mathcal{C}_{5/2}\left(\frac{\omega \pm \omega_L}{\nu_m}\right)\right]\left[1 - \frac{\omega_N^2}{\omega\nu_m}\left(\frac{\omega \pm \omega_L}{\nu_m}\right) \mathcal{C}_{3/2}\left(\frac{\omega \pm \omega_L}{\nu_m}\right)\right]^{-1/2}$$

$$+\cdots(\text{higher order terms}) \quad . \qquad (2.13)$$

Since

$$5/2\,\frac{\omega_N^2}{\omega\nu_m}\,\mathcal{L}_{5/2}\left(\frac{\omega \pm \omega_L}{\nu_m}\right) << 1 - \frac{\omega_N^2}{\omega\nu_m}\left(\frac{\omega \pm \omega_L}{\nu_m}\right)\,\mathcal{L}_{3/2}\left(\frac{\omega \pm \omega_L}{\nu_m}\right) \approx 1,$$

the higher order terms can be neglected, and the real and imaginary parts can be equated.

$$n_{o,x}^r = \left[1 - \frac{\omega_N^2}{\omega\nu_m}\left(\frac{\omega \pm \omega_L}{\nu_m}\right)\,\mathcal{L}_{3/2}\left(\frac{\omega \pm \omega_L}{\nu_m}\right)\right]^{1/2} \tag{2.14}$$

$$n_{o,x}^i = 5/4\,\frac{\omega_N^2}{\omega\nu_m}\,\mathcal{L}_{5/2}\left(\frac{\omega \pm \omega_L}{\nu_m}\right)$$

The real part can again be expanded by the binomial theorem.

$$n_o^r = 1 - \frac{\omega_N^2}{2\omega\nu_m}\left(\frac{\omega + \omega_L}{\nu_m}\right)\,\mathcal{L}_{3/2}\left(\frac{\omega + \omega_L}{\nu_m}\right) \tag{2.15}$$

$$n_x^r = 1 - \frac{\omega_N^2}{2\omega\nu_m}\left(\frac{\omega - \omega_L}{\nu_m}\right)\,\mathcal{L}_{3/2}\left(\frac{\omega - \omega_L}{\nu_m}\right) \tag{2.16}$$

The imaginary part of each mode is given by

$$n_o^i = 5/4\,\frac{\omega_N^2}{\omega\nu_m}\,\mathcal{L}_{5/2}\left(\frac{\omega + \omega_L}{\nu_m}\right) \tag{2.17}$$

$$n_x^i = 5/4\,\frac{\omega_N^2}{\omega\nu_m}\,\mathcal{L}_{5/2}\left(\frac{\omega - \omega_L}{\nu_m}\right) \tag{2.18}$$

If the change in phase can be measured over the path that the wave travels, the electron concentration can be calculated for the medium. For partial reflection, however, the reflection process must be considered. Expressions for the electron concentration when reflection is included will be developed next.

3. THE THEORY OF PARTIAL REFLECTIONS

The basis for the partial-reflection experiment is the reflection process in the D region. The incident wave is partially reflected as opposed to totally reflected. An understanding of the effects of the ionosphere on the wave as it passes through the ionosphere and as it is reflected is essential to the method.

The nature of the reflections has been a subject of considerable study. Gardner and Pawsey used the Fresnel reflection theory which was also used by Belrose and Burke. The volume scattering theory of Booker (1959) was proposed by Flood (1968) as a better description of the reflection mechanism. Several investigators have studied the characteristics of partial reflections, for instance, Gregory and Vincent (1970) and Fraser and Vincent (1970). The heights of reflection and phase path changes, respectively, were investigated to gain further insight into the nature of the partial reflections. The two principal theories will be discussed here as they apply to differential phase measurements.

3.1 Fresnel Reflection Theory

Assume a horizontally-stratified ionosphere where layers of different refractive indices constitute the stratifications. Furthermore, the refractive index changes from n to n + Δn in a distance small compared to the wavelength of operation. Therefore, the reflection coefficient from a boundary between two regions of refractive indices n_1 and n_2 is given by (Belrose and Burke, 1964)

$$R = \frac{n_2 - n_1}{n_2 + n_1} \approx \frac{\delta n}{2n} \qquad (3.1)$$

if

$$\frac{\omega_N^2}{\omega^2} \ll 1 .$$

By differentiating the quasi-longitudinal approximation to the complex refractive index (2.11) with respect to N, the reflection coefficients for the ordinary and extraordinary waves are given by

$$R_o = - \frac{\delta N e^2}{2 n_o m \varepsilon_o \omega \nu_m} \left[\left(\frac{\omega + \omega_L}{\nu_m} \right) \mathcal{L}_{3/2}\left(\frac{\omega + \omega_L}{\nu_m} \right) + j\, 5/2\, \mathcal{L}_{5/2}\left(\frac{\omega + \omega_L}{\nu_m} \right) \right]$$

$$R_x = - \frac{\delta N e^2}{2 n_x m \varepsilon_o \omega \nu_m} \left[\left(\frac{\omega - \omega_L}{\nu_m} \right) \mathcal{L}_{3/2}\left(\frac{\omega - \omega_L}{\nu_m} \right) + j\, 5/2\, \mathcal{L}_{5/2}\left(\frac{\omega - \omega_L}{\nu_m} \right) \right] . \qquad (3.2)$$

The refractive indices are both close to one; therefore, n_x will be approximately equal to n_o.

The part of the reflection coefficient which enters into the differential phase relations is the phase change due to reflection. The ordinary reflection coefficient can be expressed as

$$R_o = |R_o| \, e^{j\gamma_o} \qquad (3.3)$$

where γ_o is the phase shift that occurs due to reflection. By using equations (3.2) and (3.3), the phase γ_o can be written as

$$\gamma_o = \tan^{-1} \left[5/2 \, \mathcal{L}_{5/2}\left(\frac{\omega + \omega_L}{\nu_m} \right) \Big/ \left(\frac{\omega + \omega_L}{\nu_m} \right) \mathcal{L}_{3/2}\left(\frac{\omega + \omega_L}{\nu_m} \right) \right] \qquad (3.4)$$

Similarly, for the extraordinary wave the reflection coefficient is

$$R_x = |R_x| \, e^{j\gamma_x} \tag{3.5}$$

where

$$\gamma_x = \tan^{-1}\left[5/2 \, \mathfrak{C}_{5/2}\left(\frac{\omega - \omega_L}{\nu_m}\right) \Big/ \left(\frac{\omega - \omega_L}{\nu_m}\right) \mathfrak{C}_{3/2}\left(\frac{\omega - \omega_L}{\nu_m}\right)\right] . \tag{3.6}$$

The expressions for γ_o and γ_x are dependent on collision frequency and not on the electron concentration.

For an electromagnetic wave that is transmitted vertically from the ground, reflected from a discontinuity, and received back at the ground, Equation (2.5) becomes

$$\vec{E} = R \, \vec{\mathfrak{E}} \exp[-j\vec{k} \cdot \vec{r}] \tag{3.7}$$

where R is the reflection coefficient. Since the wave traverses the same path twice, the magnitude of the propagation vector in the $\hat{z}$ direction becomes

$$k_z = \frac{4\pi f}{c} \int_{\ell} n dz . \tag{3.8}$$

By inserting the phase of the reflection coefficient for each magneto-ionic mode into (2.10), the total phase difference is given by

$$\Delta\phi = \frac{2\omega}{c} \int_0^h (n_o^r - n_x^r) dz + (\gamma_x - \gamma_o) . \tag{3.9}$$

If $\Delta\phi$ is measured at two different altitudes h_1 and h_2, the difference between the two measurements is given by

$$\Delta\phi_2 - \Delta\phi_1 = \frac{2\omega}{c}\int_{h_1}^{h_2}(n_o^r - n_x^r)dz + (\gamma_x - \gamma_o)_2 - (\gamma_x - \gamma_o)_1 \tag{3.10}$$

where $h_2 > h_1$ and the subscripts refer to quantities at h_1 and h_2, respectively. Since the medium can be assumed to be nearly homogeneous between h_1 and h_2 if the difference between h_1 and h_2 is small, the integral in (3.10) can be approximated by

$$\frac{4\pi f}{c}\int_{h_1}^{h_2}\Delta n^r\,dz \approx \frac{4\pi f}{c}\,\Delta n^r \cdot \Delta z \tag{3.11}$$

Δz is the difference in heights, $h_2 - h_1$. From the substitution of the difference in the real parts of the refractive index given by

$$\Delta n^r = n_o^r - n_x^r = 1/2\,\frac{Ne^2}{m\varepsilon_o\omega\nu_m}\left[\left(\frac{\omega - \omega_L}{\nu_m}\right)\mathcal{G}_{3/2}\left(\frac{\omega - \omega_L}{\nu_m}\right) - \left(\frac{\omega + \omega_L}{\nu_m}\right)\mathcal{G}_{3/2}\left(\frac{\omega + \omega_L}{\nu_m}\right)\right] \tag{3.12}$$

into Equation (3.10), an expression for the electron concentration as a function of collision frequency and differential phase can be written. The electron concentration N is given by

$$N = \frac{mc\varepsilon_o\nu_m}{e^2\Delta z}\,\frac{[(\Delta\phi_2 - \Delta\phi_1) - (\gamma_x - \gamma_o)_2 + (\gamma_x - \gamma_o)_1]}{\left[\left(\frac{\omega - \omega_L}{\nu_m}\right)\mathcal{G}_{3/2}\left(\frac{\omega - \omega_L}{\nu_m}\right) - \left(\frac{\omega + \omega_L}{\nu_m}\right)\mathcal{G}_{3/2}\left(\frac{\omega + \omega_L}{\nu_m}\right)\right]} \tag{3.13}$$

Expected values of the phase difference $(\Delta\phi_2-\Delta\phi_1)$ can be calculated using a model ionosphere. The electron-concentration profiles for rockets 14.244, 14.246, and 14.247 (Figure 3.1) were used to calculate the reflection coefficient difference $\gamma_o-\gamma_x$ and the change in phase difference $\Delta\phi_2-\Delta\phi_1$. The corresponding collision-frequency profiles used for these calculations were given by Lodato and Mechtly (1971). The operating frequency used in the calculations is 2.66 MHz. Figure 3.2 shows the phase change due to reflection as a function of altitude. The variation in the phase difference due to reflection for these collision frequencies is small. In Figure 3.3 the expected values of $\Delta\phi$ are plotted for the same three rocket profiles. Because electron densities are low at lower altitudes, the values of $\Delta\phi$ expected at lower altitudes are near zero. At higher altitudes the phase due to the difference in refractive indices becomes large. In making differential phase measurements, then, one would expect to obtain $(\Delta\phi_2 - \Delta\phi_1)$ versus altitude profiles similar to those in Figure 3.3.

3.2 Volume Scattering Theory

The theory of volume scattering has been proposed as an improved model for partial reflections. Flood (1968) first applied volume scattering theory to the D-region partial-reflection experiment. He was able to calculate electron concentrations from differential absorption using this theory. For their differential phase measurements, von Biel, et al. (1970) used volume scattering theory for calculating electron concentrations. In addition, the results of their measurements were offered as evidence that the volume scattering theory was more accurate than the simpler Fresnel theory.

In contrast to Fresnel theory, the electromagnetic waves incident on the ionosphere are backscattered by a volume of random fluctuations in refractive index. For experimental calculations the size of the volume is taken to be the

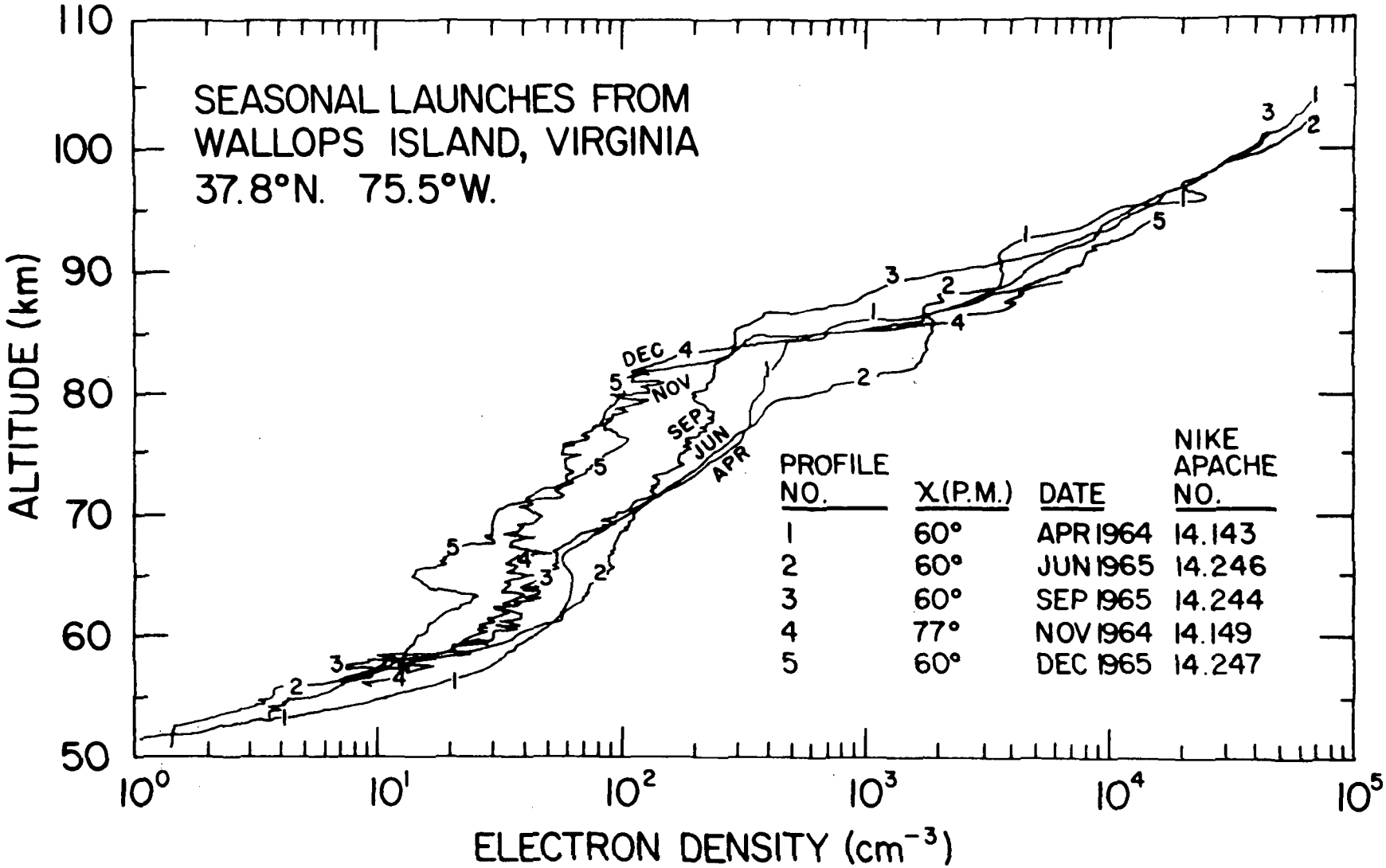

Figure 3.1 Electron concentration profiles from rocket measurements (after Mechtly and Smith, 1968)

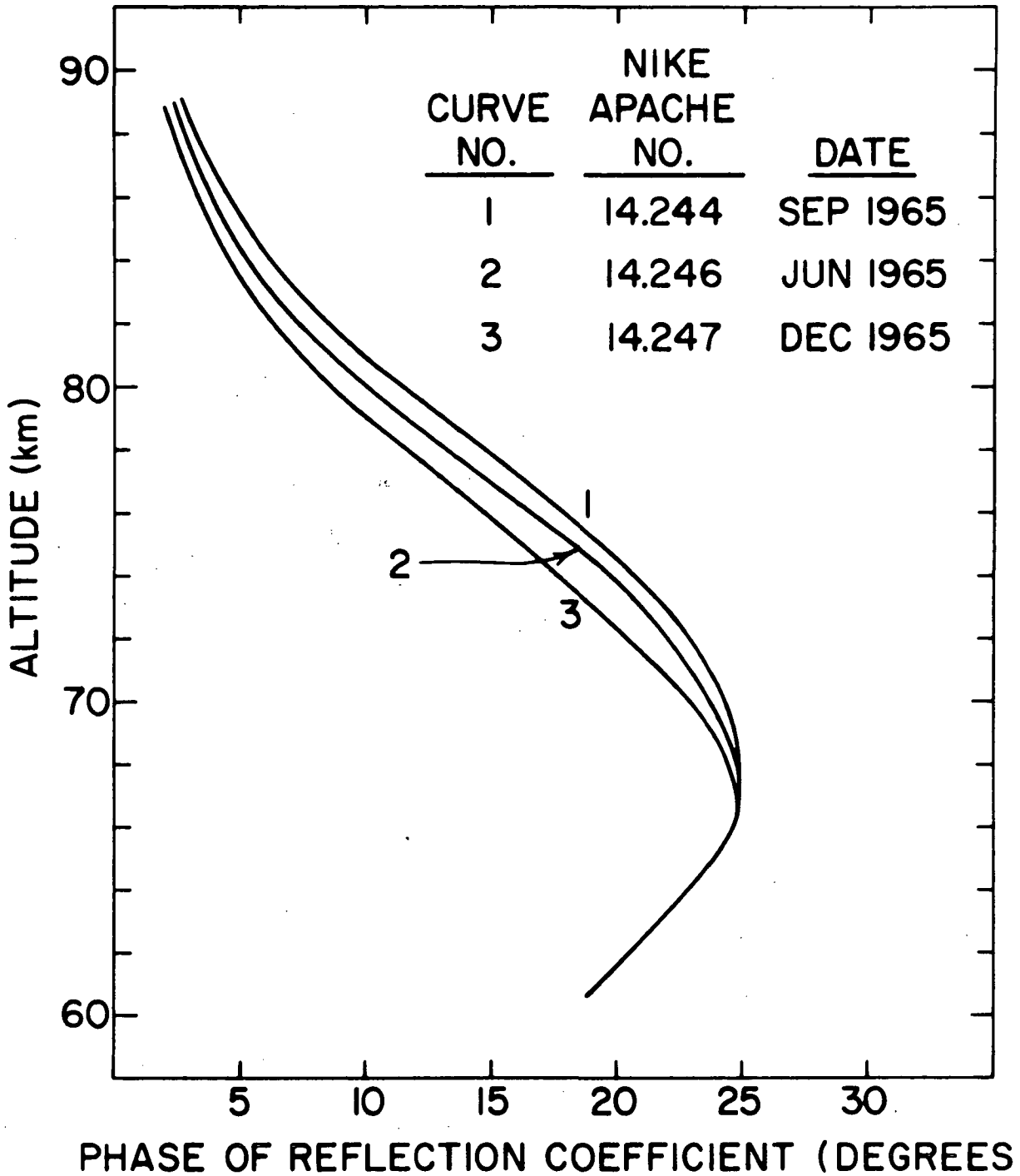

Figure 3.2 Difference between phase components of the reflection coefficients calculated from rocket measurements

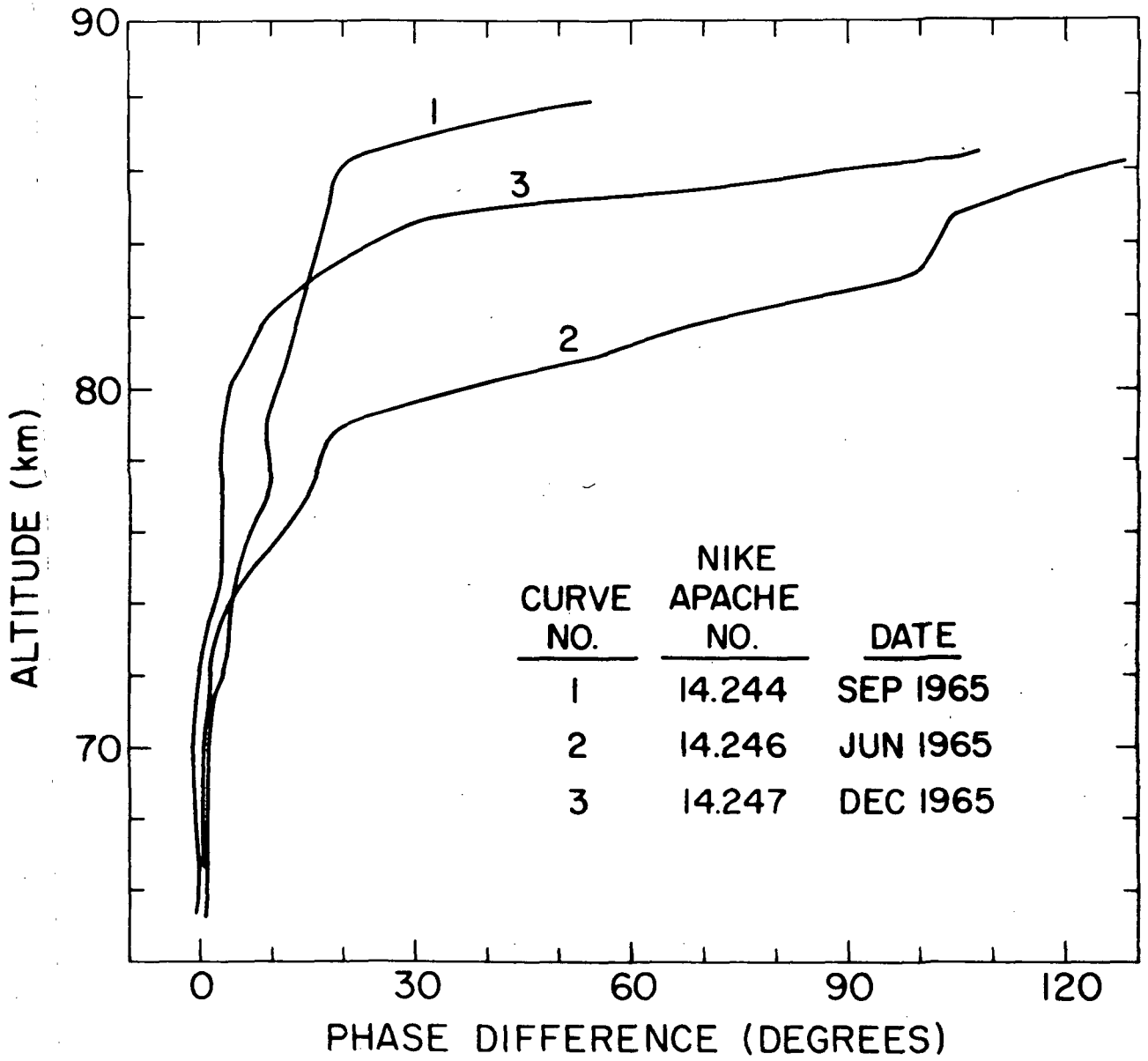

Figure 3.3 Phase difference versus altitude calculated from electron concentration profiles measured by rockets

product of the area defined by the antenna beamwidth and the resolution length of the transmitter pulse, $c\tau/2$. The important contribution of volume scattering is that the changes in refractive index throughout the scattering volume are not negligible as assumed in Fresnel theory but affect the absorption and phase of the scattered wave.

In the experiment of von Biel, et al. (1970), an expression for the correlation of the complex electric field intensities of each magneto-ionic mode was given as the starting point. For the purpose of comparing the two theories the conjugate of the expression for the correlation coefficient given by von Biel will be used here.

$$\rho(h) = \frac{\langle E_o E_x^* \rangle}{(\langle |E_o|^2 \rangle \langle |E_x|^2 \rangle)^{1/2}} \tag{3.14}$$

where the angle brackets denote ensemble averages. The correlation coefficient can be separated into its real and imaginary parts. The ratio of the imaginary part to the real part can be taken from von Biel, et al. (1970)

$$\frac{\rho^i(h)}{\rho^r(h)} = \tan\left[\frac{4\pi}{\lambda}\int_o^h (n_o^r - n_x^r)dz + \beta(h)\right] \tag{3.15}$$

The term $\beta(h)$ includes the effects on radio waves due to backscatter from the ionosphere. $\beta(h)$ is given by

$$\beta(h) = (\gamma_x - \gamma_o) + \frac{\Delta}{\xi} - \frac{\sin(\alpha\Delta)\exp(-\alpha\xi)}{1 - \cos(\alpha\Delta)\exp(-\alpha\xi)} \tag{3.16}$$

where γ_o and γ_x are the phase of the reflection coefficients defined in (3.3) through (3.6)

$$\Delta = n_x^r - n_o^r$$

$$\xi = n_x^i + n_o^i$$

$$\alpha = 2\pi c\tau/\lambda$$

τ = transmitted pulse length in seconds.

Only the last term of (3.16) is a function of the pulse length τ. The limit of the last term as τ approaches zero can be found by using L'Hospital's rule.

$$\lim_{\tau \to 0} \frac{\sin(\alpha\Delta)\exp(-\alpha\xi)}{1.0 - \cos(\alpha\Delta)\exp(-\alpha\xi)} = \frac{\Delta}{\xi} \quad . \tag{3.17}$$

Therefore, in the limit as τ approaches zero Equation (3.15) becomes

$$\frac{\rho^i(h)}{\rho^r(h)} = \frac{2\omega}{c} \int_o^h (n_o^r - n_x^r)dz + (\gamma_x - \gamma_o) \quad . \tag{3.18}$$

The right hand side of this expression is identical to that of Equation (3.9). The above derivation is a check on the expressions derived from Fresnel theory since the two theories should give the same result as the pulse length becomes close to zero.

In order to implement a differential phase system to calculate electron concentrations a reflection model must be chosen. The electron-density profiles of von Biel, et al. (1970) and von Biel (1971) were calculated using volume scattering theory. The complexity of the expressions necessitates the use of iterative techniques to determine electron concentrations. The Fresnel model will be used here because of the simpler expression for electron density. While there may be some question as to which theory gives the best results, the Fresnel theory will give results sufficiently accurate to evaluate the system.

4. DIFFERENTIAL PHASE MEASURING SYSTEM

A method for measuring the phase difference between the ordinary and extraordinary modes was developed by Parkinson (1955) and later improved by Ferraro (1959) to study the polarization of ionospherically-reflected LF waves. A similar method was applied to differential phase partial-reflection measurements by von Biel, et al. (1970). Two orthogonal antennas in the $\hat{x}$ and $\hat{y}$ directions ($\hat{x} \times \hat{y} = \hat{z}$) are fed such that the amplitude and phase of the wave to each antenna can be controlled. If the amplitudes are equal and the phase of the wave in one antenna leads the other by 90°, the antennas can transmit and receive circularly polarized waves. Both right and left circular polarization can be obtained in this manner. If the waves are in phase at the antennas with equal amplitudes or if only one antenna is fed, the resulting polarization will be linear. The measured values are amplitudes. When these amplitudes are combined in the proper way, the phase change due to ionization in the D region can be evaluated.

Parkinson (1955) and Ferraro (1959) used a method of calculation which utilizes the angle of phase difference between the ordinary and extraordinary waves. On the other hand, von Biel, et al. (1970) calculated a correlation coefficient. Both methods give the same result, as will be shown; however, each method can give different insight into the measurement.

4.1 Angle of Phase Difference

The complex intensity of the backscattered field from a height h is

$$\vec{E} = \vec{E}_o + \vec{E}_x = \frac{A_o}{\sqrt{2}} (\hat{x} + j\hat{y}) + \frac{A_x}{\sqrt{2}} (\hat{x} - j\hat{y}) \qquad (4.1)$$

The transmitted wave is linearly polarized and pulsed. Mode coupling and oblique echo effects are assumed to be negligible. From (4.1) the electric vector of the ordinary ray as a function of time [exp(-jωt)] is

$$\vec{E}_o = \frac{A_x}{\sqrt{2}} (\hat{x} \cos\omega t + \hat{y} \sin\omega t) \quad . \tag{4.2}$$

Similarly,

$$\vec{E}_x = \frac{A_x}{\sqrt{2}} [\hat{x} \cos(\omega t + \phi) - \hat{y} \sin(\omega t + \phi)] \tag{4.3}$$

is the electric vector of the extraordinary ray. Both the ordinary and extraordinary rays experience a phase shift due to ionization and reflection. However, since only the total phase difference ϕ is needed, ϕ is added to the argument of the extraordinary mode while the phase of the ordinary wave is referenced to zero. The angle ϕ is the quantity to be measured.

The angle ϕ is measured by combining the amplitudes of received partial reflections for a suitable set of polarizations. Let

A_o - Ordinary wave transmission and reception

A_x - Extraordinary wave transmission and reception

The next four amplitudes are received following a linearly polarized transmission.

A_1 - Linearly polarized reception in $\hat{x}$ direction

A_2 - Linearly polarized reception in $\hat{y}$ direction

A_3 - Linearly polarized reception midway between $\hat{x}$ and $\hat{y}$ directions

A_4 - Linearly polarized reception midway between $-\hat{x}$ and $\hat{y}$ directions

The voltage V_1 at the terminals of the receiving antenna oriented in the $\hat{x}$ direction is

$$V_1 = \frac{A_o}{\sqrt{2}} \cos\omega t + \frac{A_x}{\sqrt{2}} \cos(\omega t + \phi) \quad . \tag{4.4}$$

The amplitude is

$$A_1^2 = \left[\frac{A_o}{\sqrt{2}} + \frac{A_x}{\sqrt{2}} \cos\phi\right]^2 + \left[\frac{A_x}{\sqrt{2}} \sin\phi\right]^2 = \frac{A_o^2}{2} + \frac{A_x^2}{2} + A_o A_x \cos\phi \quad . \tag{4.5}$$

Similarly for the receiving antenna oriented in the $\hat{y}$ direction the amplitude is

$$A_2^2 = \frac{A_o^2}{2} + \frac{A_x^2}{2} - A_o A_x \cos\phi \tag{4.6}$$

at this point, by measuring A_o, A_x, A_1, and A_2, an expression for the angle ϕ can be obtained by taking the difference between A_1^2 and A_2^2

$$\cos\phi = (A_1^2 - A_2^2)/(2A_o \cdot A_x) \tag{4.7}$$

The sum of A_1^2 and A_2^2 is

$$A_1^2 + A_2^2 = A_o^2 + A_x^2 \quad . \tag{4.8}$$

Expressing $\cos\phi$ as

$$\cos\phi = 1/2\left[\frac{A_1^2 - A_2^2}{A_1^2 + A_2^2}\right] \cdot \left[\frac{A_o^2 + A_x^2}{A_o \cdot A_x}\right] \tag{4.9}$$

gives a relation which is independent of system gain changes between circular and linear polarizations.

If the polarization of the receiving antenna is rotated such that it is polarized in a direction midway between $\hat{x}$ and $\hat{y}$, the angle ϕ is effectively increased by $\pi/2$. Therefore, the electric vectors are

$$\vec{E}_o = A_o[\hat{x}\cos\omega t + \hat{y}\sin\omega t]/\sqrt{2}$$

$$\vec{E}_x = A_x[\hat{x}\cos(\omega t + \phi + \pi/2) - \hat{y}\sin(\omega t + \phi + \pi/2)]/\sqrt{2}\ . \qquad (4.10)$$

The voltage from the x component is given by

$$V_3 = \frac{A_o}{\sqrt{2}}\cos\omega t + \frac{A_x}{\sqrt{2}}\cos(\omega t + \phi + \pi/2) \qquad (4.11)$$

The amplitude is given by

$$A_3^2 = \frac{A_o^2}{2} + \frac{A_x^2}{2} - A_o A_x \sin\phi\ . \qquad (4.12)$$

By orienting the polarization midway between $-\hat{x}$ and $\hat{y}$, the angle ϕ is effectively increased by $\frac{3\pi}{2}$. The amplitude of the fourth polarization is given by

$$A_4^2 = \frac{A_o^2}{2} + \frac{A_x^2}{2} + A_o A_x \sin\phi \qquad (4.13)$$

Again an expression for the angle ϕ can be found by taking the difference between A_3^2 and A_4^2

$$\sin\phi = \frac{(A_4^2 - A_3^2)}{2 A_o \cdot A_x} \quad . \tag{4.14}$$

By inserting the sum of A_3^2 and A_4^2 into (4.14) as was done in (4.9),

$$\sin\phi = 1/2\left[\frac{A_4^2 - A_3^2}{A_4^2 + A_3^2}\right] \cdot \left[\frac{A_o^2 + A_x^2}{A_o \cdot A_x}\right] \quad . \tag{4.15}$$

Equations (4.9) and (4.15) are sufficient to find ϕ, provided the amplitudes are sampled sufficiently close together. However by taking

$$\tan\phi = \frac{\sin\phi}{\cos\phi} = \frac{\left[\dfrac{A_4^2 - A_3^2}{A_4^2 + A_3^2}\right]}{\left[\dfrac{A_1^2 - A_2^2}{A_1^2 + A_2^2}\right]} \tag{4.16}$$

and retaining the signs of $\sin\phi$ and $\cos\phi$, the difficulty of locating the correct quadrant is eliminated.

Von Biel, et al. (1970) have derived (4.9) and (4.15) in terms of the correlation of the ordinary and extraordinary backscattered fields. The correlation coefficient (Equation 3.14) is given by

$$\rho(h) = \frac{\langle E_o E_x^* \rangle}{(\langle |E_o|^2 \rangle \ \langle |E_x|^2 \rangle)^{1/2}} \tag{4.17}$$

where the angle brackets denote ensemble averages. From Equation (4.1), A_1 and A_2 can be written as the voltages in the $\hat{x}$ and $\hat{y}$ directions, respectively.

$$A_1 = \frac{A_x}{\sqrt{2}} + \frac{A_o}{\sqrt{2}}$$

$$A_2 = j\left(\frac{A_o}{\sqrt{2}} - \frac{A_x}{\sqrt{2}}\right) \tag{4.18}$$

Solving for A_o and A_x in terms of A_1 and A_2,

$$A_o = \frac{\sqrt{2}}{2}(A_1 - j\,A_2)$$

$$A_x = \frac{\sqrt{2}}{2}(A_1 + j\,A_2) \tag{4.19}$$

Substituting equations (4.19) into (4.17),

$$\frac{\langle A_o A_x^* \rangle}{(\langle A_o^2 \rangle \cdot \langle A_x^2 \rangle)^{1/2}} = \frac{\left\langle \left[\frac{\sqrt{2}}{2}(A_1 - j\,A_2) \cdot \frac{\sqrt{2}}{2}(A_1 - j\,A_2)\right]\right\rangle}{(\langle A_o^2 \rangle \cdot \langle A_x^2 \rangle)^{1/2}}$$

$$= \frac{1/2(\langle A_1^2 \rangle - \langle A_2^2 \rangle) - j\langle A_1 A_2 \rangle}{(\langle A_o^2 \rangle \cdot \langle A_x^2 \rangle)^{1/2}} \tag{4.20}$$

Amplitudes A_3 and A_4 can be written from their definitions.

$$A_3 = \frac{\sqrt{2}}{2} A_1 + \frac{\sqrt{2}}{2} A_2$$

$$A_4 = -\frac{\sqrt{2}}{2} A_1 + \frac{\sqrt{2}}{2} A_2 \tag{4.21}$$

Solving for A_1 and A_2 and taking the product,

$$A_1 \cdot A_2 = \frac{1}{\sqrt{2}} (A_3 + A_4) \cdot \frac{1}{\sqrt{2}} (A_3 - A_4)$$

$$= \frac{1}{2} (A_3^2 - A_4^2) \qquad (4.22)$$

Separating (4.20) into its real and imaginary components,

$$\rho^r(h) = \frac{1}{2} \left[\frac{\langle A_1^2 \rangle - \langle A_2^2 \rangle}{\langle A_1^2 \rangle + \langle A_2^2 \rangle} \right] \cdot \left[\frac{\langle A_o^2 \rangle + \langle A_x^2 \rangle}{(\langle A_o^2 \rangle \cdot \langle A_x^2 \rangle)^{1/2}} \right]$$

$$\rho^i(h) = \frac{1}{2} \left[\frac{\langle A_4^2 \rangle - \langle A_3^2 \rangle}{\langle A_4^2 \rangle + \langle A_3^2 \rangle} \right] \cdot \left[\frac{\langle A_o^2 \rangle + \langle A_x^2 \rangle}{(\langle A_o^2 \rangle \cdot \langle A_x^2 \rangle)^{1/2}} \right] \qquad (4.23)$$

again since,

$$A_o^2 + A_x^2 = A_1^2 + A_2^2 = A_3^2 + A_4^2 \qquad (4.24)$$

the expressions (4.23) have been written as ratios in order to eliminate errors due to system gain changes. Equations (4.23) are identical to Equations (4.9) and (4.15).

4.2 Differential Phase Measuring System

The partial-reflection differential phase measuring system is diagrammed in block form in Figure 4.1. The system is a modified version of the one used by Pirnat and Bowhill (1968), Reynolds and Sechrist (1970), and Birley and Sechrist

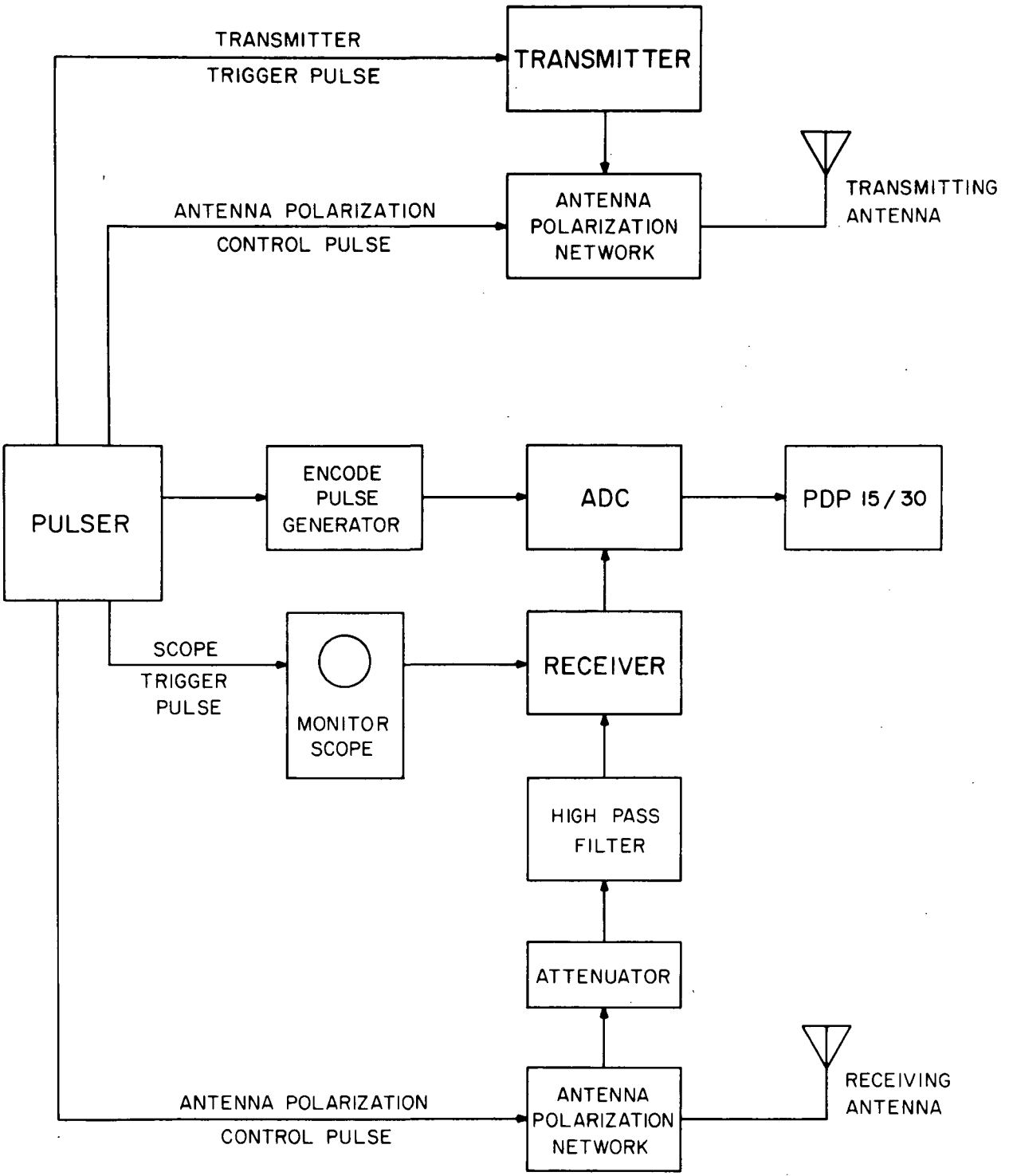

Figure 4.1 Block diagram of differential phase partial reflection system

(1971). Much of the detail of the equipment such as the receiver and transmitter has been described by Henry (1966).

Pulser

The pulser controls the system by synchronizing the various components of the system. Two pulses 33 milliseconds apart are supplied to trigger the transmitter, control the polarizations of the polarization networks, and initiate the computer data collection. The repetition rate for the set of two pulses is variable, but is generally at 1.25 sets per second.

Transmitter

The transmitter operates at a frequency 2.66 MHz in a pulsed mode. The pulse width is continuously variable, but is usually set at 50μs or 25μs. The output power of the transmitter is 40 kilowatts.

Transmitter Antenna Polarization Network

Figure 4.2 is a block diagram of the network designed to polarize the antennas. The amplitudes of the polarizations desired--A_o, A_x, A_1, A_2, A_3, and A_4--were described previously and their corresponding polarizations are illustrated in Figure 4.4. The transmitter power is delivered to a divider (Figure 4.2) which sends one half of the signal to each feed line. An attenuator in each line equalizes the power that will be delivered to the respective antennas. To obtain circular polarization as required for the ordinary (A_o) and extraordinary (A_x) modes, a pair of crossed dipoles must be fed with waves 90° out of phase with each other. A 180° phase shift in an antenna feed line will give circular polarization in the opposite direction. If the 90° phase delay is deleted, linear polarization results. The direction of linear polarization is controlled manually. With the phase delay deleted and power fed to both antennas, the polarization is directed northwest as required to obtain A_1 and A_2. With the west-east antennas deleted

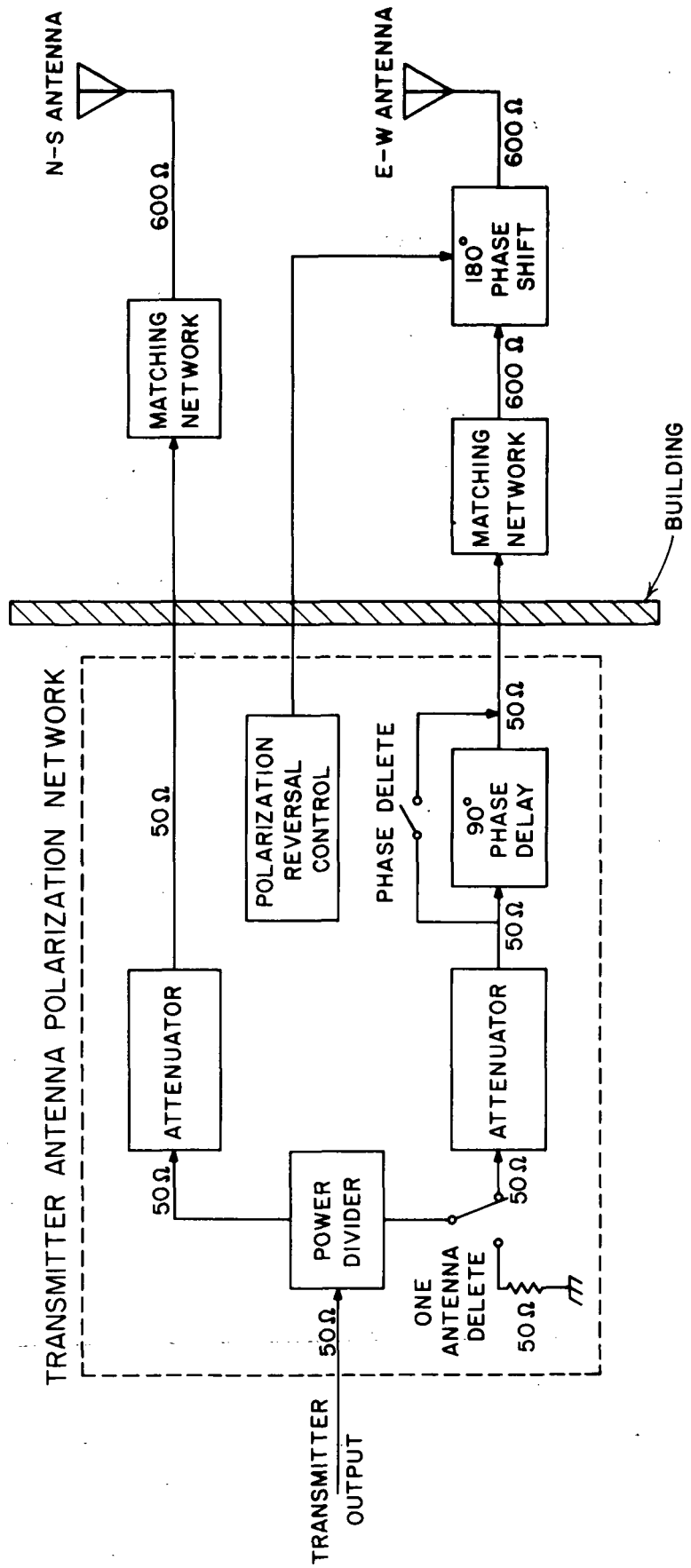

Figure 4.2 Differential phase transmitter antenna polarization network

the polarization is directed towards the north, for A_3 and A_4.

Antennas

Two large antenna arrays, one for transmitting and one for receiving, are used in the partial-reflection system. Each antenna consists of a grid of 60 half-wave dipoles, 30 in the north-south direction and 30 in the east-west direction. The gain is directed vertically with a calculated 3dB beamwidth of 14°.

Receiver Antenna Polarization Network

The network used to polarize the receiving antennas is diagrammed in Figure 4.3. The operation of the receiving network is similar to that of the transmitter polarization network. A manual phase delete switch has been added to obtain linear polarization. Figure 4.4 shows the directions of polarization during reception. For the first linear polarization (A_1), the direction of polarization is north-west. A 180° phase shift of the north-south antenna changes the direction to south-west, which gives the required direction for reception of A_2. The direction of polarization for A_3 and A_4 is identical to that of A_1 and A_2, respectively.

Receiver

A solid-state, superheterodyne receiver is used in the partial-reflection system. The center frequency is at 2.66 MHz with a bandwidth of about 40 MHz. The gain is about 80 dB. Provision is made for adjusting the RF and IF gain separately. A manually-switched attenuator is used in front of the receiver to attenuate signals that would otherwise saturate the receiver. A high-pass filter with a cutoff frequency of 1.9 MHz is used to eliminate interference from local broadcast stations. An oscilloscope is used to monitor the partial reflections at the receiver output.

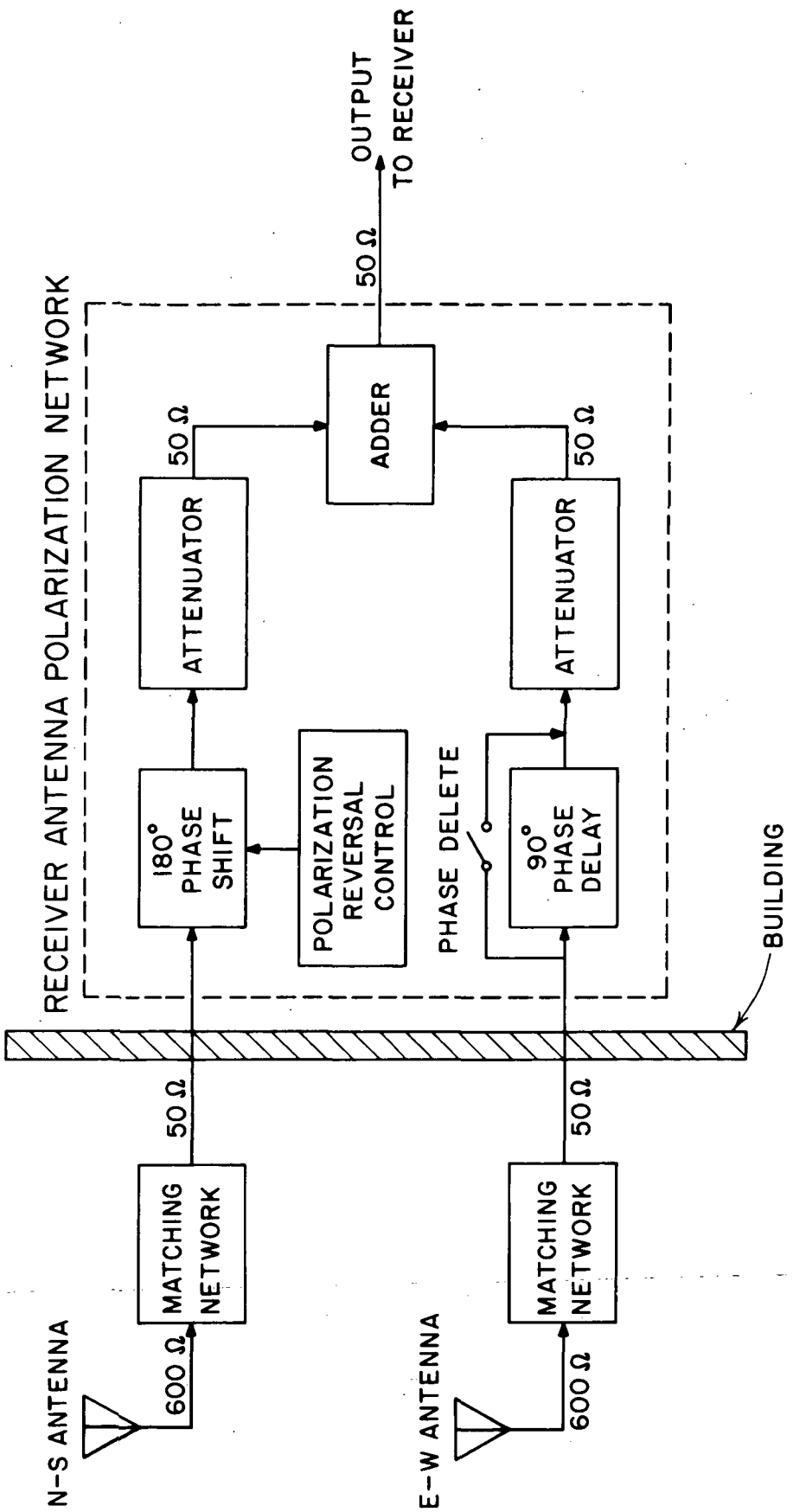

Figure 4.3 Differential phase receiver antenna polarization network

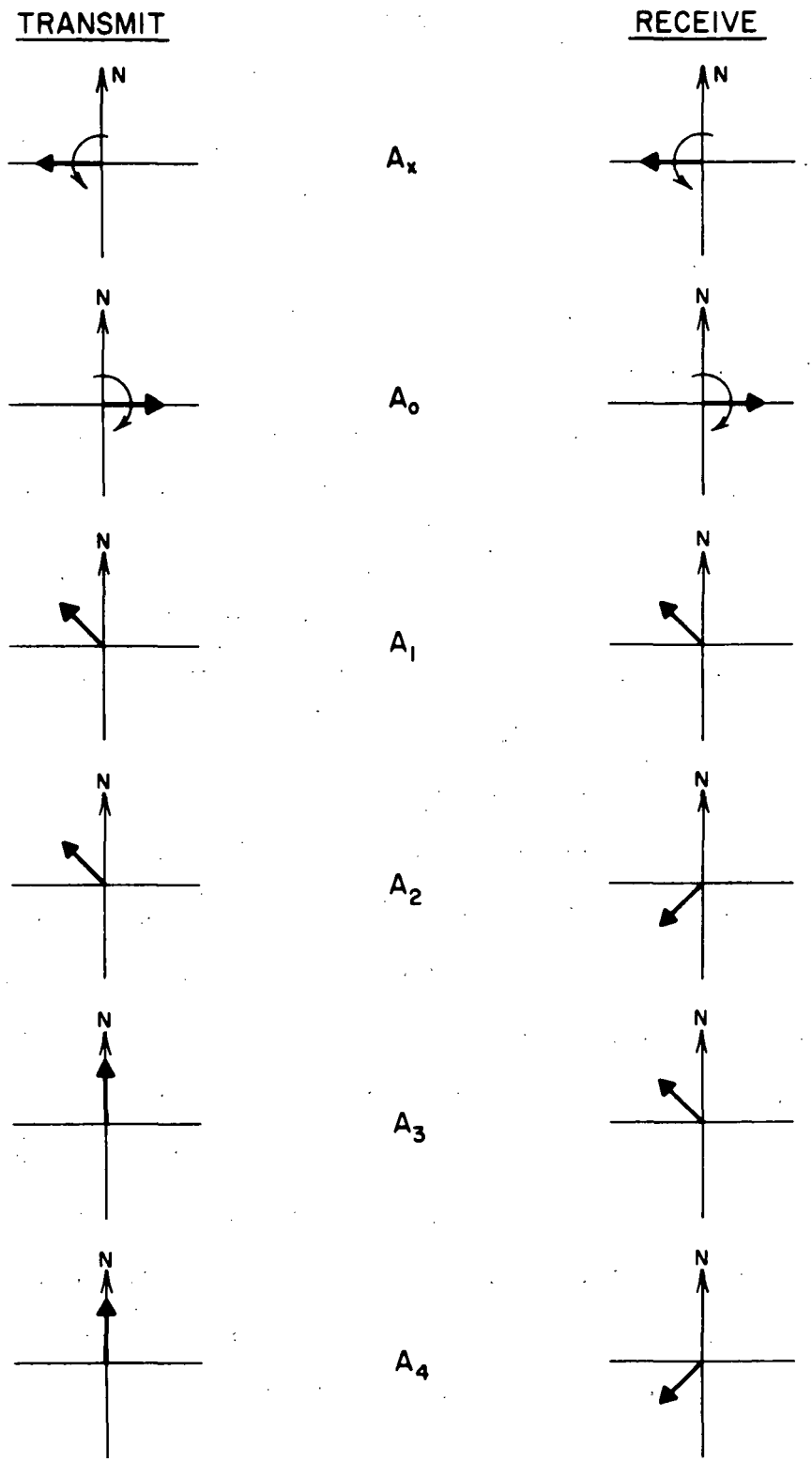

Figure 4.4 Antenna polarizations required to obtain the amplitudes A_o, A_x, A_1, A_2, A_3, and A_4

Analog-to-Digital Converter and Computer

An HP5610A analog-to-digital converter (ADC) digitizes the dc output of the receiver. Sampling at a rate of 100 kHz, the ADC has a height resolution of 1.5 kilometers. The ADC has a voltage resolution of 9 bits for an input voltage range of from 0 to 1.0 volts. An encode pulse generator, which is triggered by the pulser, gates the ADC such that it digitizes the voltages for the heights of interest.

A PDP 15/30 small computer is used to store and process data. The computer has 16K words of core where each word consists of 18 bits. Data are stored on DECtapes and can be processed at a later time. Most of the programming is done in FORTRAN with the exception of some special programming which must be done in MACRO or assembly language. A more complete description of the computer and its peripherals was presented by Birley and Sechrist (1971).

Data Collection and Processing Programs

Data are collected from the partial-reflection system through the use of the computer program, DLOGD. Each pulse from the pulser generates a frame of samples which are digitized by the ADC and stored in memory. Each frame consists of four noise samples where no partial reflections are expected and 21 signal samples, covering the altitude range from 60 to 90 kilometers in 1.5 kilometer increments. Two frames, for example, one for the ordinary mode and one for the extraordinary mode, constitute a set. When nine sets are present in memory, the data are written out on DECtape for storage and later processing. This sequence is repeated until a sufficient number of samples have been collected.

Processing is controlled by MASTER. MASTER handles input-output instructions from the operator that allow him to select the files to be used and dictate how the data are to be processed. MASTER calls the subroutine PROAXD which does the bulk of the processing. PROAXD reads the values of the data off the DECtape and

calculates the mean square of the amplitudes. Noise is extracted from the signal using the noise samples taken during data collection according to the following scheme

$$A_S = \sqrt{A_{S+N}^2 - A_N^2}$$

where

A_S is the amplitude of the signal;

A_{S+N} is the amplitude of the signal plus noise; and

A_N is the amplitude of the noise.

The average values of the amplitudes for A_o, A_x, A_1, A_2, A_3, and A_4 for each height are stored in memory. PROAXD, then, calls subroutines to calculate electron concentrations from the ratios of A_x to A_o (see Birley and Sechrist, (1971), for a description and listing of the subroutines). DIFASE is called by MASTER to use Equations (4.16) and (4.23) for obtaining the desired phase difference angles and correlation coefficients. The electron concentration, as expressed in Equation (3.13) is calculated by a straightforward FORTRAN program called PHELD.

Operation of the System

Data are collected over a 15-minute period. The collection period is divided into three 5-minute segments. During the first segment the polarization shift networks are set for circular polarizations and the amplitudes of the ordinary and extraordinary modes are collected and stored in one data file. During the second 5-minute segment, the 90° phase delays in both polarization networks are deleted manually. Two linear polarizations (A_1 and A_2) are collected and written on a second data file. During the final segment, one part of the

transmitting antenna is switched to a dummy load, changing the direction and amplitude of the polarization. The remaining two polarizations (A_3 and A_4) are then recorded on a third data file. Three hundred seventy-eight samples of each of the six amplitudes are compiled over the entire collecting period. The data are then ready for processing.

5. RESULTS OF DIFFERENTIAL PHASE MEASUREMENTS

The objective of making differential phase partial-reflection measurements is to obtain electron-concentration profiles of the D region. In this chapter several profiles will be presented to demonstrate the results of the technique. The data collection period began on October 13, 1971, and continued through November 5, 1971. The location of the system is northeast of Urbana, Illinois at geographic coordinates: 40°N, 88°W.

The advantage of making differential phase measurements by the system described in Chapter 4 is that differential absorption measurements are made simultaneously. Comparisons can be made quite readily of the results from the two techniques. A common collision-frequency profile was chosen for calculating electron concentrations by both methods: this collision-frequency profile (Figure 5.1) was chosen as representative of several equinox profiles presented by Lodato and Mechtly (1971).

The phase difference, the ratio A_x/A_o, and the amplitude of the correlation coefficient are plotted as a function of altitude for two data runs in Figures 5.2 and 5.3. These phase difference profiles have the same general shape as those presented in Figure 3.3. The phase difference increases slowly at the lower altitudes, whereas at higher altitudes it increases very rapidly. The rapid increases in phase difference occur at lower altitudes for the data measured by the system than for the calculated values from the rocket data.

The amplitude of the correlation coefficient in Figures 5.2 and 5.3 is a decreasing function of altitude. This indicates that the ordinary and extraordinary waves tend to become uncorrelated as altitude increases. Ionospheric characteristics such as electron concentrations and the nature of the partial

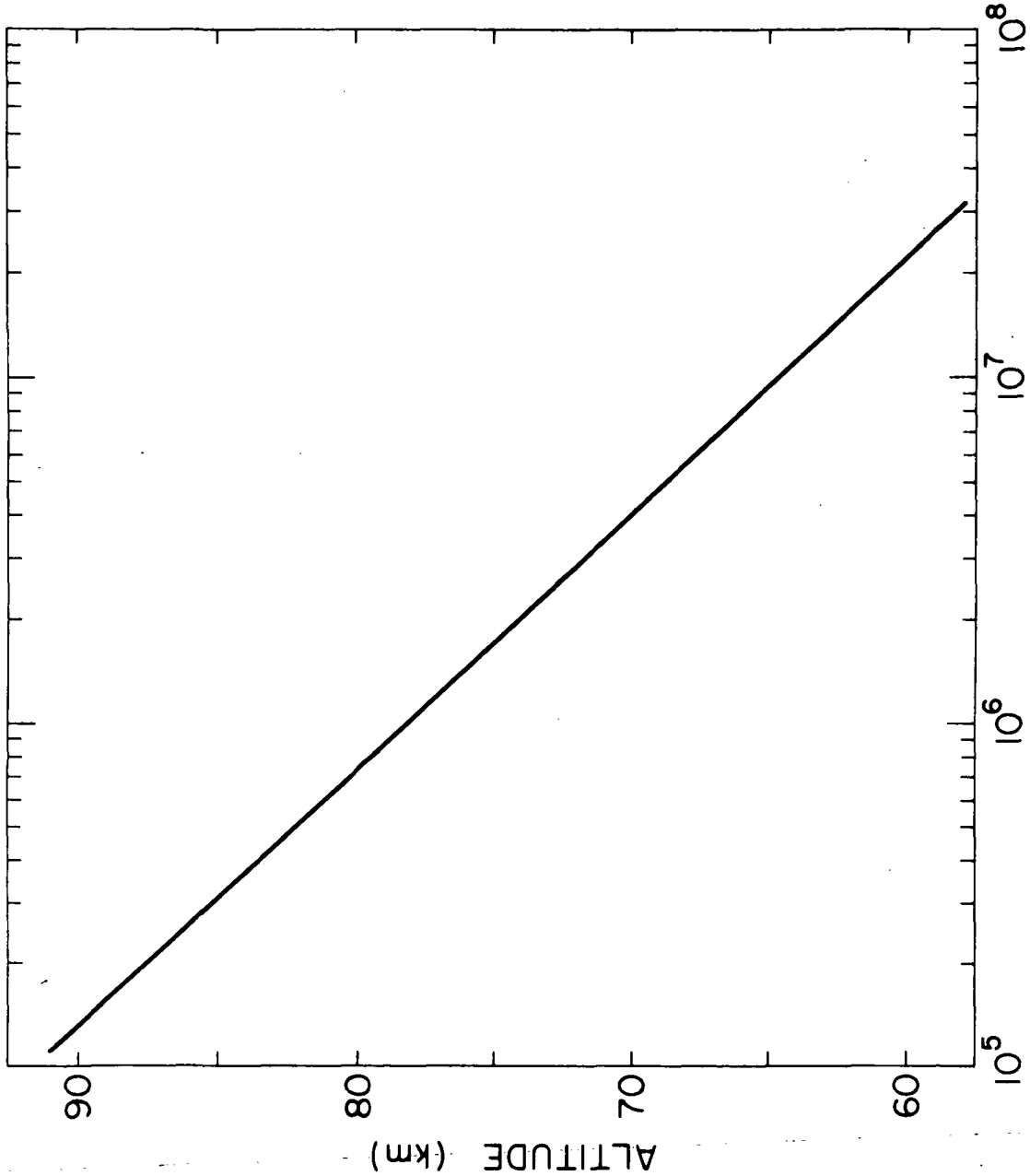

Figure 5.1 Collision frequency profile used for calculating electron concentrations from both differential phase and differential absorption

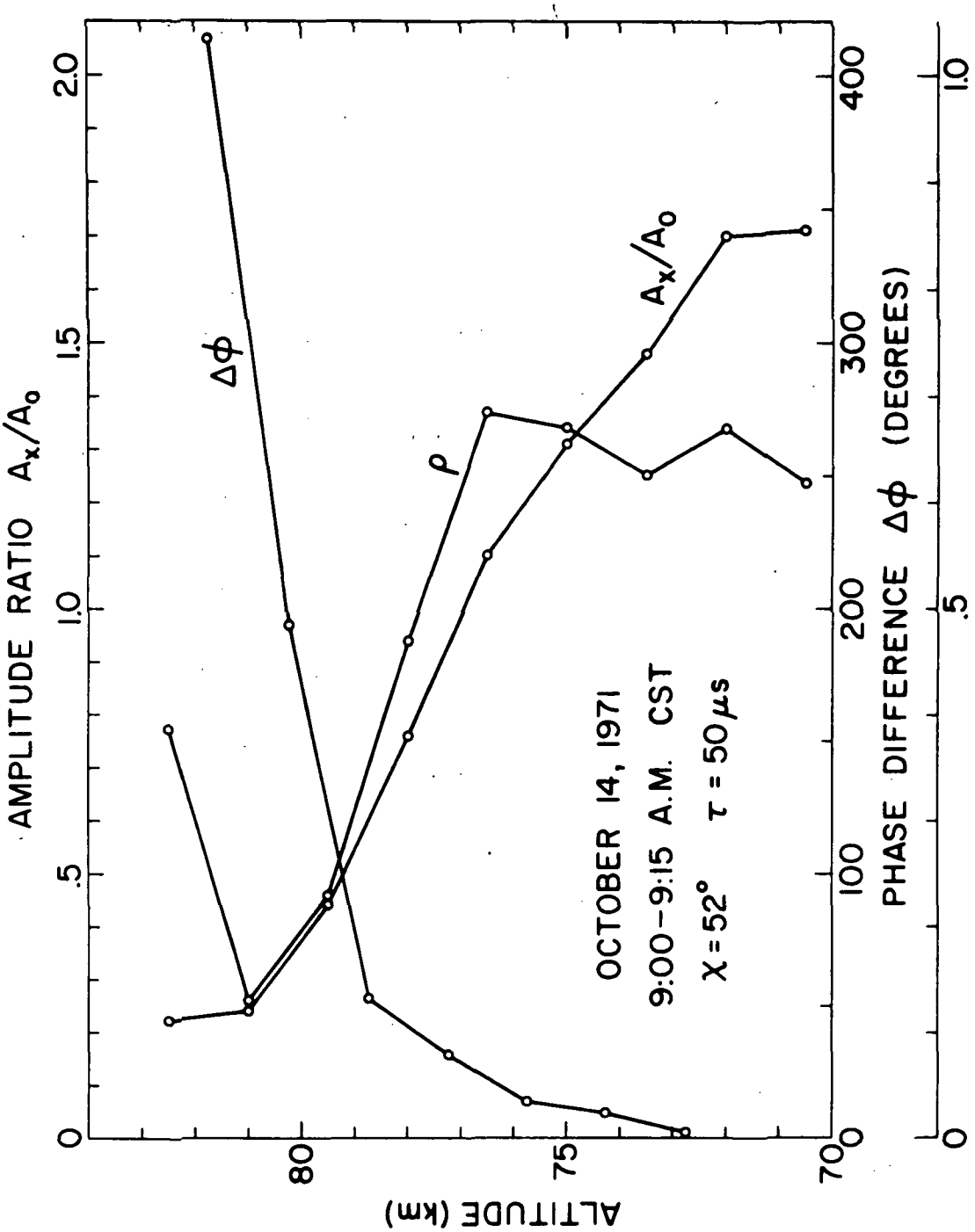

Figure 5.2 Phase difference amplitude ratio, and amplitude of the correlation coefficient versus altitude

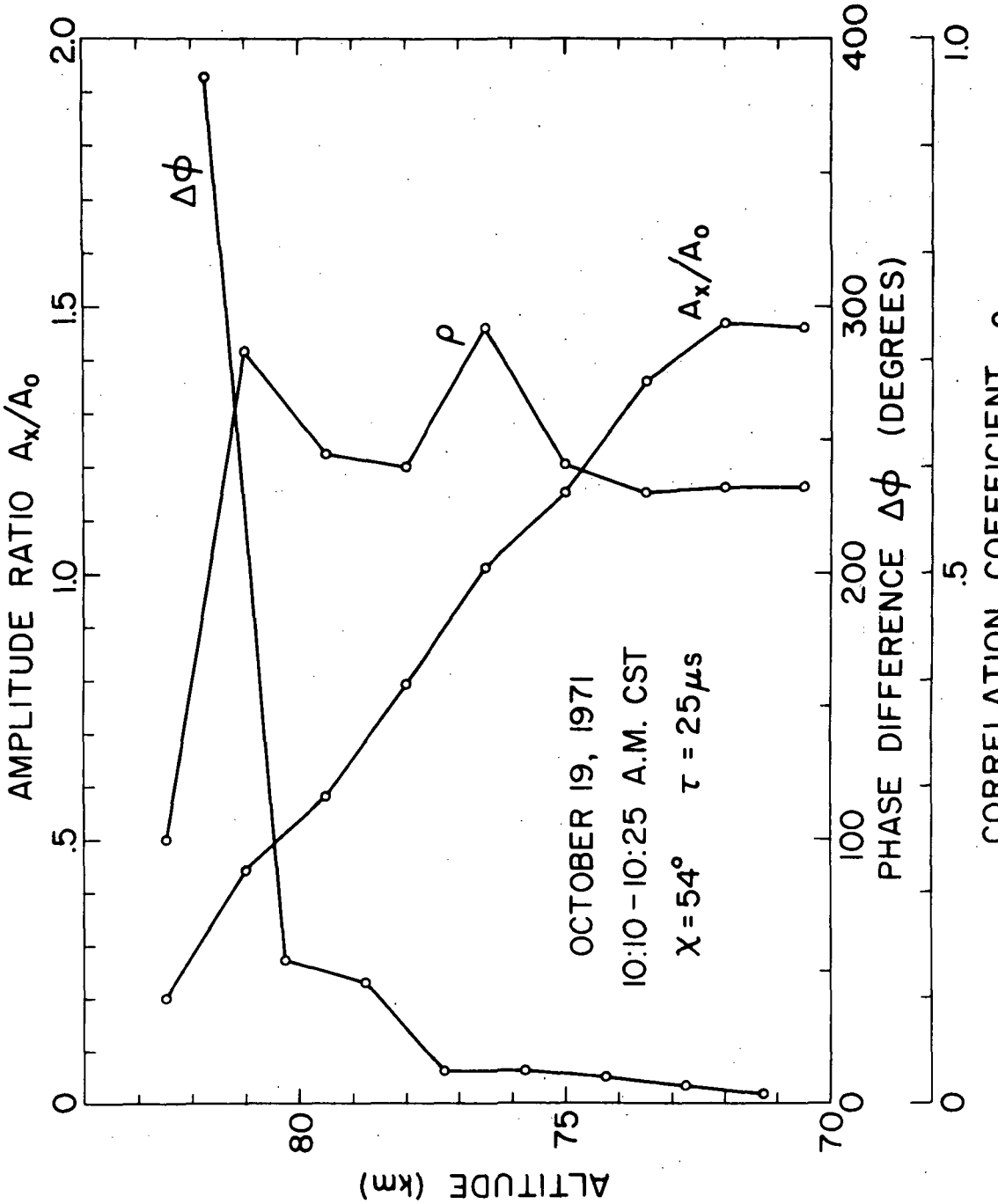

Figure 5.3 Phase difference amplitude ratio, and amplitude of the correlation coefficient versus altitude

reflections can be deduced from the correlation coefficient. From the results of von Biel, et al. (1970), one would expect the correlation coefficient to be near unity at low altitudes. The measured values of ρ were seldom larger than 0.8 below 75 kilometers. Since ρ is a function of the refractive indices of the waves, it is a function of the electron concentration. If the values of ρ are too small, the electron concentration from ρ would be too large. The correlation coefficient shows a rapid change at high altitudes as do the phase difference and A_x/A_o. The use of the amplitude of the correlation coefficient to calculate electron concentrations was suggested by von Biel (1971).

The electron-density profiles from differential phase and differential absorption are presented in Figures 5.4 through 5.10. In general, the agreement between differential phase and differential absorption results is quite good. Values of electron concentration were obtained over altitudes from 70 kilometers to 86 kilometers depending on the kind of day. In particular the profiles from absorption and phase of Figure 5.7 show good agreement over a range of 10 kilometers. The solar zenith angles were less than 60° for all of the measurements.

The length of the transmitted pusle was either 50μs or 25μs. The first runs of data were collected with a 50μs pulse. Later 25μs was tried and seemed to give somewhat better results.

The seven profiles show some variability in electron concentration over the data collection period. The values of the electron density are large at low altitudes during mid-October. Beginning with Figure 5.8 the electron density appears to have decreased. These observations are consistent with those made by the regular differential absorption measurements during this period.

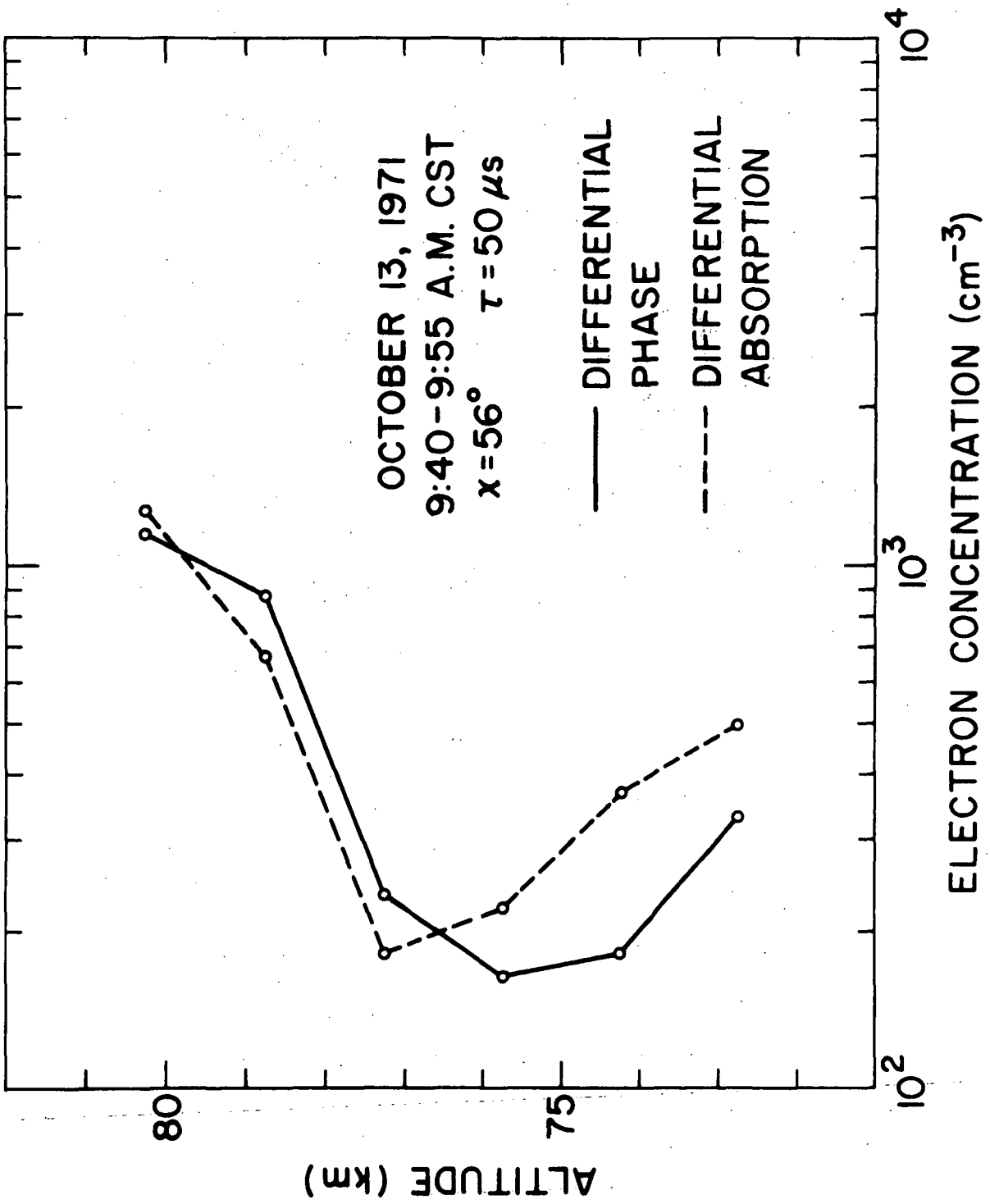

Figure 5.4 Electron concentration versus altitude from differential phase and differential absorption (October 13, 1971) $\chi = 56°$

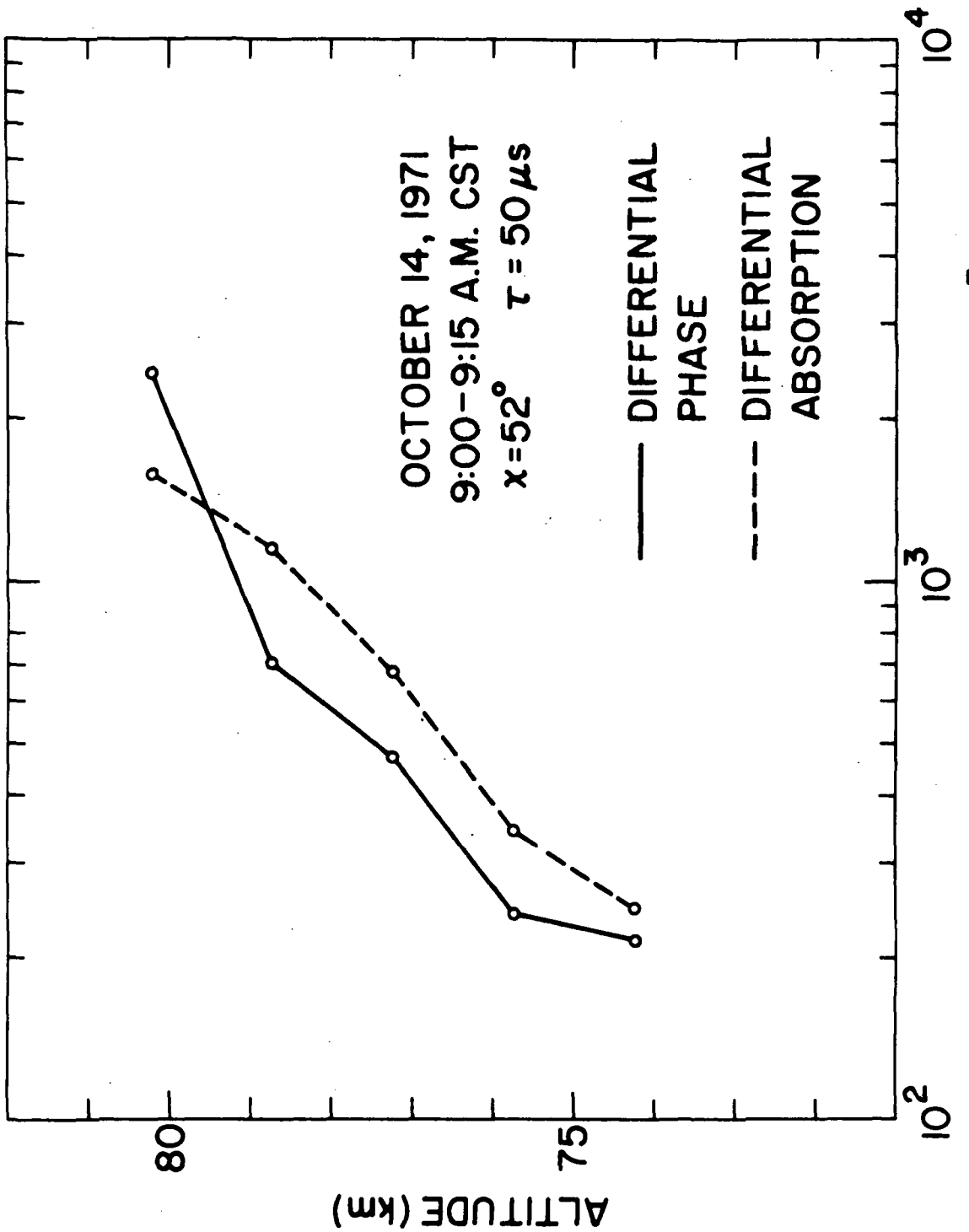

Figure 5.5 Electron concentration versus altitude from differential phase and differential absorption (October 14, 1971) $\chi = 52°$

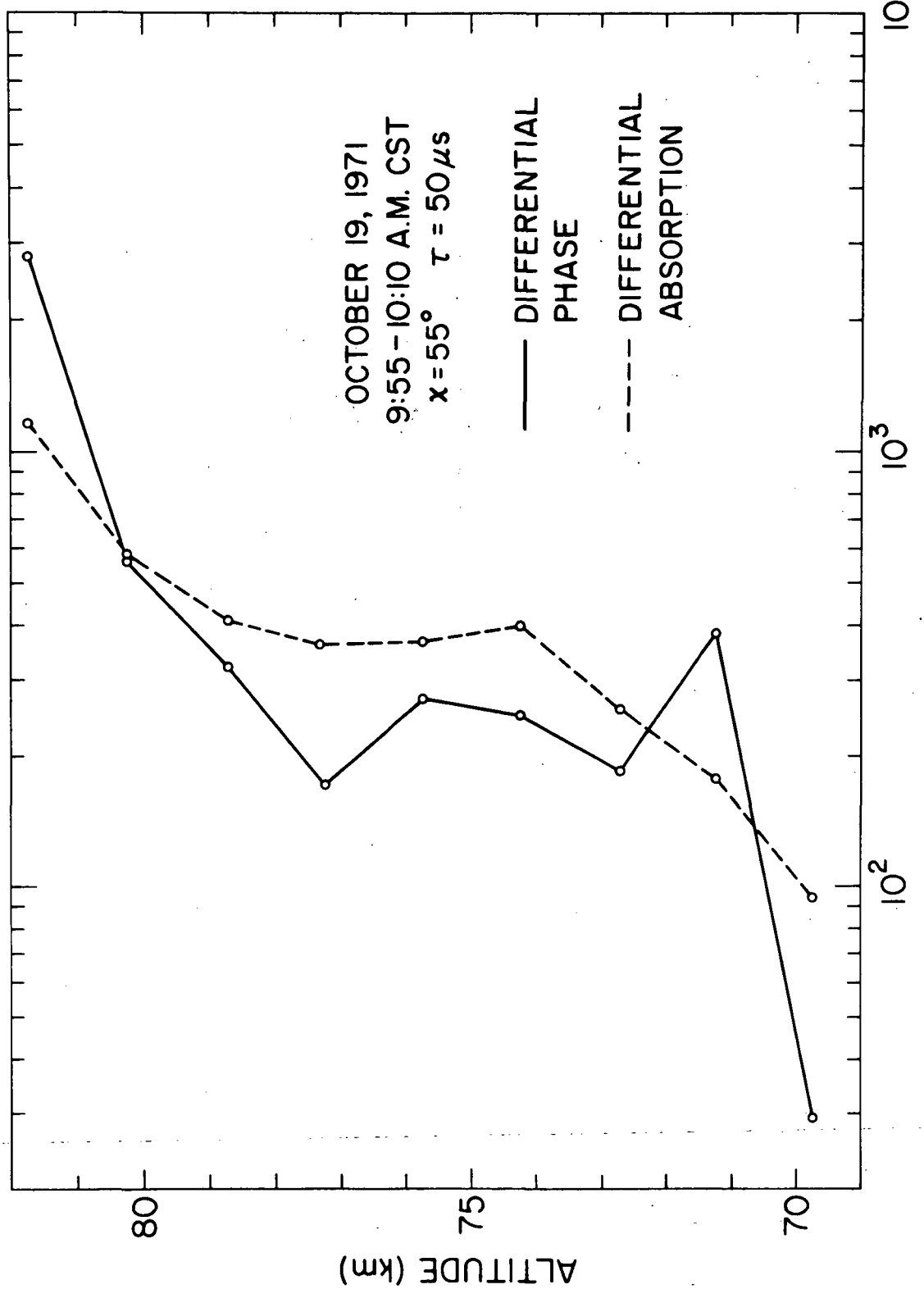

Figure 5.6 Electron concentration versus altitude from differential phase and differential absorption (October 19, 1971) $\chi = 55°$

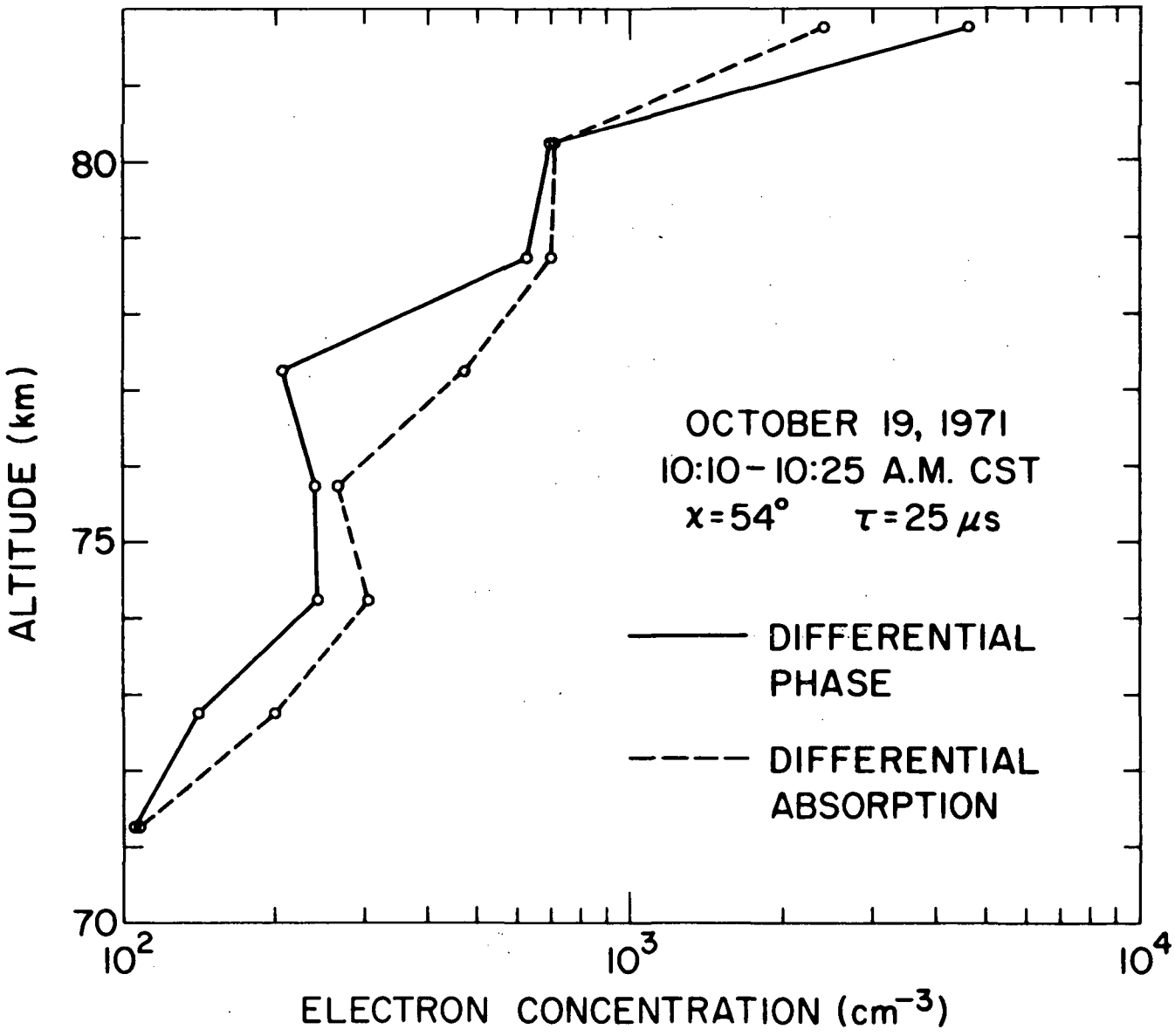

Figure 5.7 Electron concentration versus altitude from differential phase and differential absorption (October 19, 1971) χ = 54°

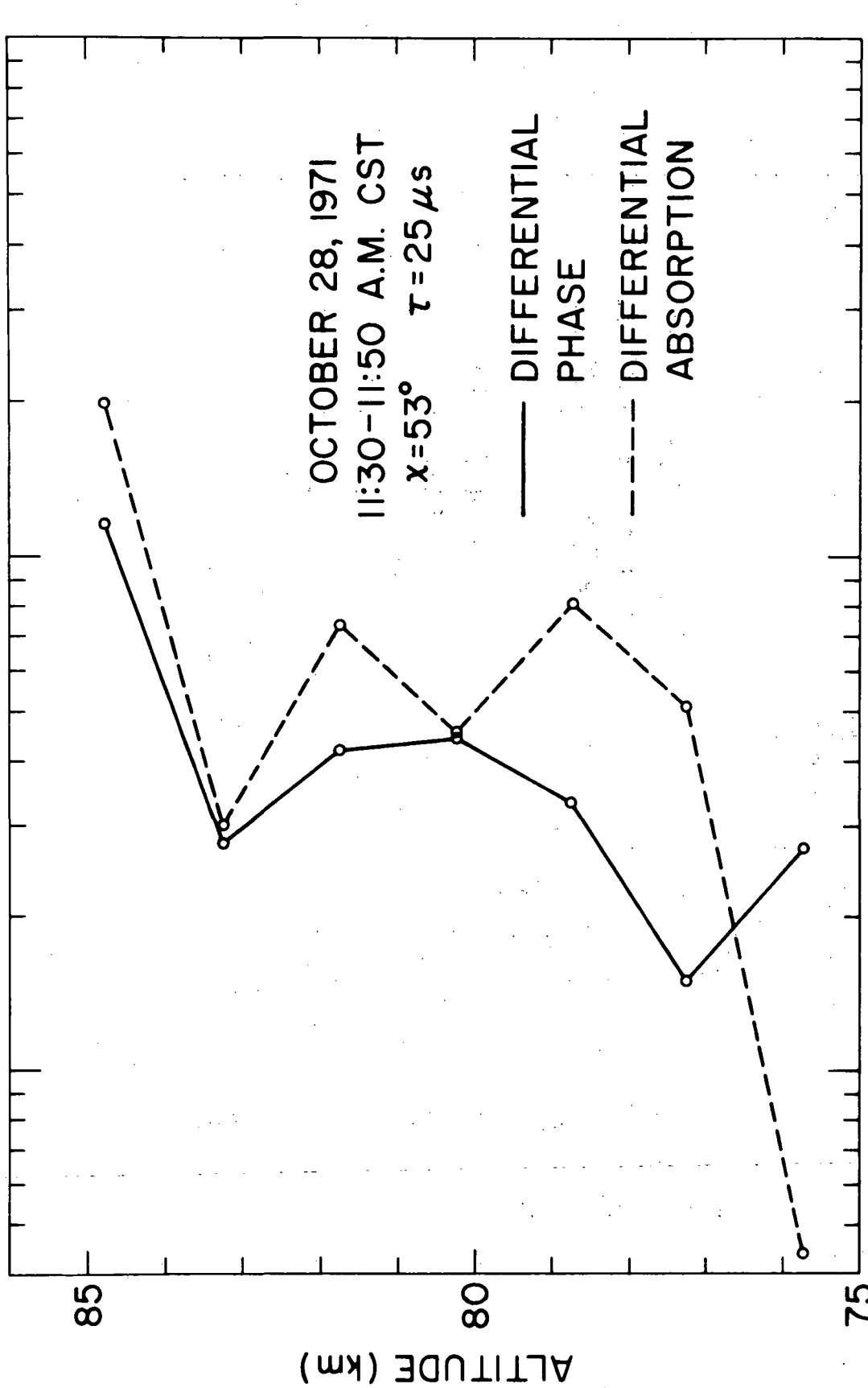

Figure 5.8 Electron concentration versus altitude from differential phase and differential absorption (October 28, 1971) $\chi = 53°$

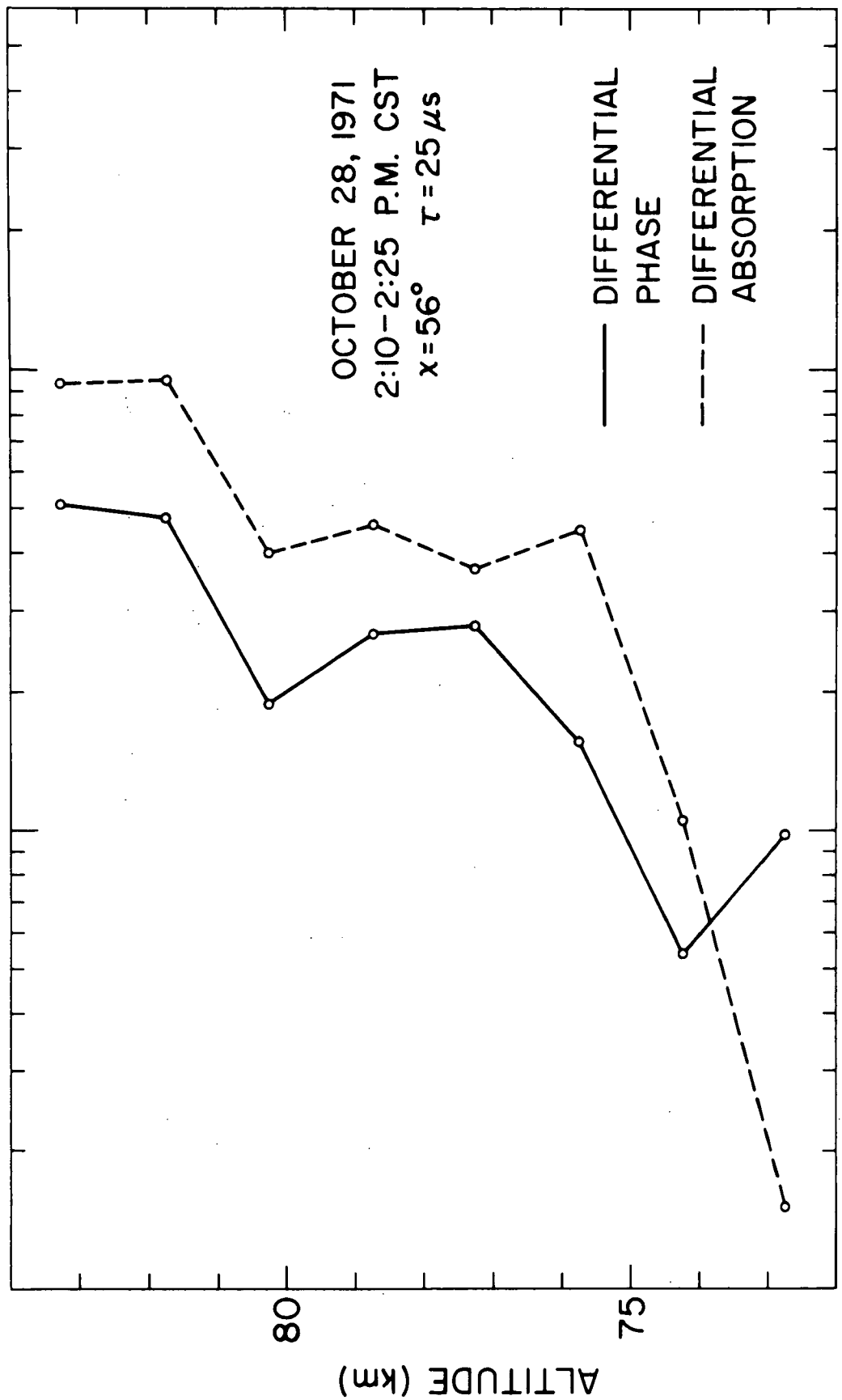

Figure 5.9 Electron concentration versus altitude from differential phase and differential absorption (October 28, 1971) χ = 56°P.M.

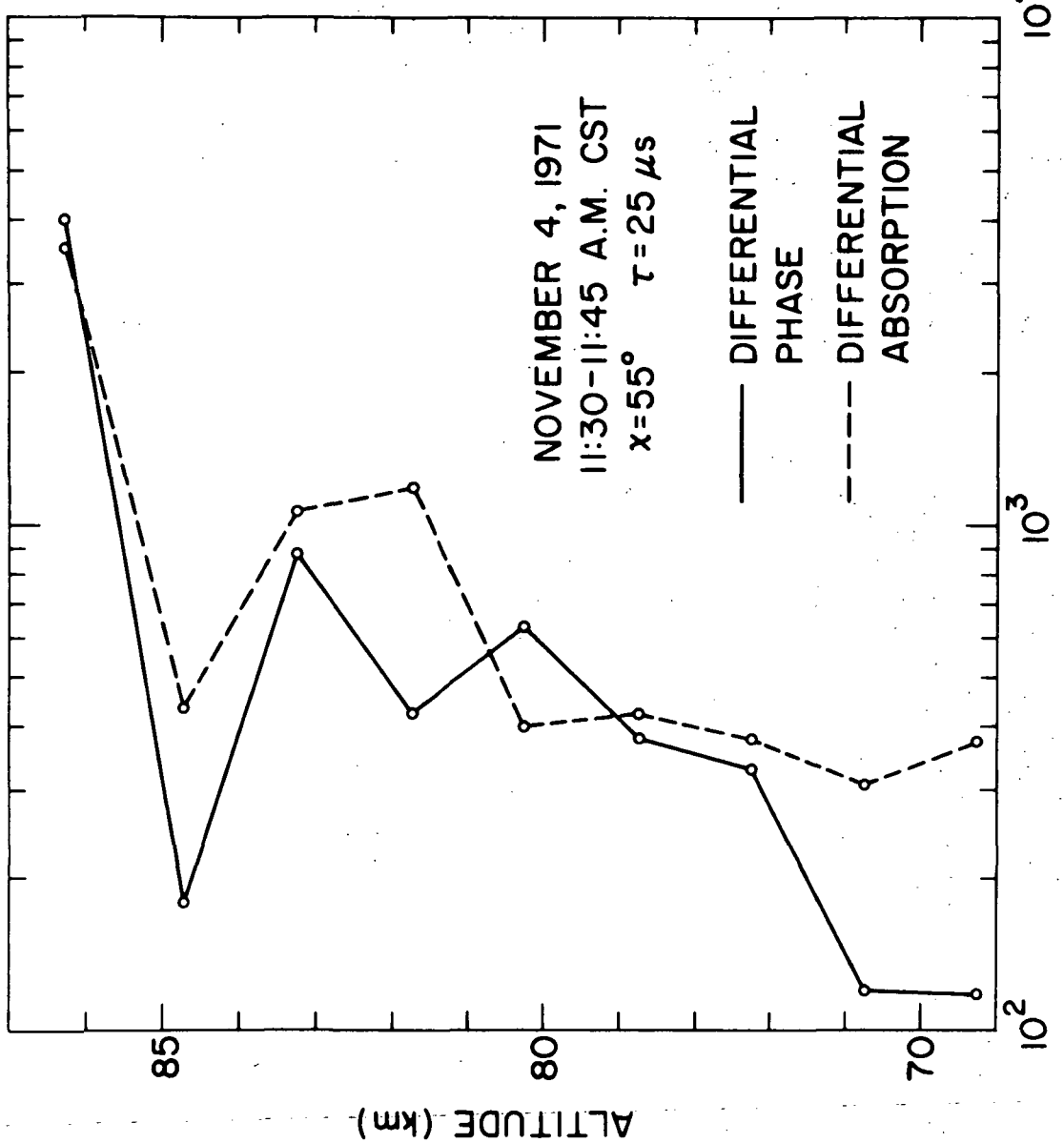

Figure 5.10 Electron concentration versus altitude from differential phase and differential absorption (November 4, 1971) $\chi = 55°$

6. DIFFERENTIAL PHASE SYSTEM EVALUATION

A differential phase partial-reflection system has been developed, and the results from it have been presented in Chapter 5. It is necessary to examine the system and the results to arrive at some quantitative conclusions as to the merits of the system. To evaluate the system, sources of error must be considered. The magnitude of these errors and their cumulative effect on the final results must be analyzed. Suggestions can then be made for minimizing the errors and improving the overall quality of the system. From this evaluation one can better understand the merits and limitations of the system.

The sources of error can be divided into two categories: those errors due to uncertainties in measuring techniques, and those due to faulty assumptions in the theoretical calculations. Several sources of error which apply to this system will be considered under each of these categories.

One of the best ways of evaluating a differential phase system is to compare the results with those from differential absorption measurements made simultaneously. This comparison has been done in Chapter 5. Further comparisons with data from other types of experiments would also be worthwhile and will be done here.

6.1 Uncertainties in Measurement Techniques

In Chapter 4 the polarizations required for each of the six amplitudes were assumed to be exactly circular or exactly linear as required. Whether or not the polarizations are really circular or linear must be considered as well as what effect the non-circular or non-linear polarizations will have on the measurement. The criteria for transmission or reception of circular polarization are that the amount of attenuation of the wave in each feedline be equal and

the wave of one feedline be 90° out of phase with respect to the wave in the other feedline. For linear polarization, the attenuation of each wave must be the same, and there must be zero phase difference between the two waves. If the wave attenuation in each feedline is different, the angle ϕ in the equations for each amplitude (4.5, 4.6, 4.12, and 4.13) has an error. Since the wave attenuation in each line can be adjusted to within 3%, the maximum possible error in ϕ is 2°. The maximum error occurs when ϕ is an odd multiple of $\pi/2$. As ϕ approaches zero the error in ϕ becomes nearly zero. Therefore, the effect of an error in the direction of polarization will not be important. A method of testing the phase between the two feedlines is to measure the rejection of one mode while transmitting the other mode. Each antenna had a rejection of 20 dB for both modes. If for linear polarizations the phase between the two feedlines is not zero, the polarizations will be elliptical. Again the possible error is less than 2°, if the phase difference between the feedlines is less than one degree.

The output of the receiver is non-linear. If this non-linearity remained in the data, the changes in ϕ over height would be significantly affected. A computer program which approximates the receiver output by a piece-wise linear curve compensates for the non-linearity.

When the gain of the receiver is set for measuring partial reflections at low altitudes, the signals from the stronger reflections at higher altitudes saturate the receiver. If the data from saturated signals are accepted, the mean squared amplitude will be too low. Therefore, samples that saturate the receiver must be rejected. PROAXD rejects saturated signals and lists the number of rejections for each amplitude. If the number of rejections at a particular altitude is significant, that is, on the order of 10% of the samples, the data are considered to be invalid.

The timing of the control pulses in the system is very important for the precise determination of altitude. The center of the transmitted pulse is taken as the zero height. Signals from 60 kilometers and 90 kilometers are received 400 and 600 μs later, respectively. An error of 6.67 μs will result in a height error of one kilometer. The present system can be adjusted such that the height error is no more than two kilometers.

The noise which can contaminate the data can be either internal or external. The internal noise in the system is very low. External noise such as atmospherics or interference can be very significant. When a received signal is contaminated by a large source such as a flash of lightning or a strong radio transmitter the entire frame is rejected. By sampling at about 30 kilometers the amplitude of the noise is recorded. The signal can be subtracted from the signal plus noise as described in Chapter 4. The signal-to-noise ratio was examined for each height, and data with ratios of less then 1.5 were not accepted.

Each of the six amplitudes measured at a particular height is a random number the squared value of which varies about a most probable or mean squared value. If the number of samples over time is large, the amplitudes squared will tend to a normal distribution about the mean squared value. The standard deviation can be estimated by (Carpenter and Bowhill, 1971)

$$u = \pm \left(\frac{(\langle |A_s|^2 \rangle)^2}{n} + \frac{(\langle |A_n|^2 \rangle)^2}{4n} \right)^{1/2} \qquad (6.1)$$

where $\langle |A_s|^2 \rangle$ is the mean squared amplitude of the signal, $\langle |A_n|^2 \rangle$ is the mean squared amplitude of the noise, and is the number of samples. For the data of Figure 5.5, the standard deviation is $\pm$ 5% for each amplitude.

The effect of a standard deviation on the phase difference and eventually the electron concentration will now be considered. Each of the four mean squared amplitudes in Equation (4.16) $\langle |A_i|^2 \rangle$ can be represented by a number z_i with a standard deviation u_i. We will assume that the squares of the four standard deviations are equal.

$$u_1^2 = u_2^2 = u_3^2 = u_4^2 = u^2 \tag{6.2}$$

The standard deviation of $\Delta\phi$ for Equation (4.16) is given by

$$\sigma(\Delta\phi) = \frac{1}{1 + p^2}\,\sigma(p) \tag{6.3}$$

where

$$p = \left[\frac{z_4 - z_3}{z_4 + z_3}\right] \Big/ \left[\frac{z_1 - z_2}{z_1 + z_2}\right]$$

The standard deviation of p is given by

$$\sigma(p) = \sqrt{2}\, u \left(\frac{z_1 - z_2}{z_1 + z_2}\right)\left(\frac{z_4 + z_3}{z_4 - z_3}\right) \cdot$$

$$\left[\frac{\dfrac{1}{(z_4 - z_3)^2} + \dfrac{1}{(z_4 + z_3)^2}}{\left(\dfrac{z_4 - z_3}{z_4 + z_3}\right)^4} + \frac{\dfrac{1}{(z_1 - z_2)^2} + \dfrac{1}{(z_1 + z_2)^2}}{\left(\dfrac{z_1 - z_2}{z_1 + z_2}\right)^4}\right]^{1/2} \tag{6.4}$$

The standard deviation for the phase difference between two heights is given by

$$\sigma(\Delta\phi_2 - \Delta\phi_1) = \sqrt{\sigma^2(p_2) + \sigma^2(p_1)} \tag{6.5}$$

The standard deviation of the electron density is given by

$$\sigma(N) = \frac{mc\varepsilon_o \nu m}{e^2 \Delta z} \quad \frac{\sigma(\Delta\phi_2 - \Delta\phi_1)}{\left[\left(\frac{\omega - \omega_L}{\nu_m}\right) \mathcal{E}_{3/2}\left(\frac{\omega - \omega_L}{\nu_m}\right) - \left(\frac{\omega + \omega_L}{\nu_m}\right) \mathcal{E}_{3/2}\left(\frac{\omega + \omega_L}{\nu_m}\right)\right]} . \tag{6.6}$$

These standard deviations for a u of 10% have been calculated from the data of October 19, 1971, at $\chi = 55°$ and are tabulated in Table 6.1. The standard deviations of the electron concentrations $\sigma(N)$ range from 6% at 75.75 kilometers to 24% at 80.25 kilometers.

6.2 Assumptions and Theories

In order to measure parameters of the ionosphere, one must have some knowledge of what the ionosphere is really like. Assumptions are made concerning the ionization, the collision frequency and the reflection model. If these assumptions are wrong the analysis and results will be wrong. A detailed development of these assumptions will not be attempted here, but rather a summary of the problems involved will be presented.

The best way to evaluate a system for measuring electron concentrations is to compare the results from the system with a real electron density profile. However, it is very difficult to know what the real electron density is because so few of the parameters necessary to calculate the ionization such as concen-

Table 6.1

Standard deviations calculated from data of October 19, 1971, $\chi = 55°$.

Altitude (km)	$\sigma(p)$	$\sigma(\Delta\phi)$ (Degrees)	Altitude (km)	$\sigma(\Delta\phi_2 - \Delta\phi_1)$ (Degrees)	$\sigma(N)_3$ (cm^{-3})
75.0	1.85×10^{-2}	0.466	75.75	1.84	29.2
76.5	2.78×10^{-1}	1.87	77.25	1.80	25.6
78.0	2.56×10^{-1}	0.248	78.75	5.43	72.5
79.5	1.59	5.43	80.25	12.6	154.
81.0	3.46×10^{-1}	11.4	81.75	29.6	359.
82.5	9.52	27.2			

trations of ionized and neutral species and reaction rates are known at the time of measurement. The rocket profiles are considered to be close to the real profiles; however, the number of profiles from rockets are few and the variability is great. For example, rocket profiles from 1964 through 1969 (Mechtly, 1972) show a range of 100 to 900 electrons cm^{-3} at 80 kilometers. All but two of the 20 profiles from differential phase measurements have values of electron concentration within this range at 80 kilometers.

Another factor is the change in ionization over the sampling period. This is particularly important in the case of the system used here because amplitudes A_1 and A_2 are taken 5 minutes apart from amplitudes A_3 and A_4. The change in ionization is largely dependent on the change in solar zenith angle. By minimizing the change in solar zenith angle, changes in ionization can be minimized. All of the data collected were for solar zenith angles less than or equal to 60°. Therefore, changes in solar zenith angle were on the order of one degree or less over the 15-minute collection period. If the six amplitudes could be taken simultaneously at a high pulse repetition rate, reliable measurements can be made during periods when the zenith angle is changing rapidly.

The choice of the proper theory has been considered in Chapter 3. While the two methods should give similar results, the difference in the results from the two theories may be important. The concept of the correlation coefficient introduced by von Biel et al. (1970) may prove useful for evaluating the two theories. The correlation coefficient is a measure of the relative influence of the medium on the two waves. One would expect the two waves to become uncorrelated with increasing altitude. The phase of the reflection coefficient is essentially the same as the phase difference derived from Fresnel theory. However, the magnitude of the correlation coefficient could provide useful information. Further measurements and study of the correlation coefficient are recommended.

6.3 Collision Frequency

The calculation of electron concentrations using Equation (3.12) depends on an assumed collision-frequency profile. The profile of Figure 5.1 was used to obtain the results presented in Chapter 5. One explanation for the discrepancy between the profiles from differential absorption and those for differential phase is that the assumed collision-frequency profile was incorrect.

The effect of changing the collision frequency can be demonstrated by calculating electron concentrations from the differential absorption and the differential phase expressions. A_x/A_o and $\Delta\phi$ are kept constant as the collision frequency is varied. As an example, when the collision frequencies of Figure 5.1 were doubled, the electron concentrations from differential absorption decreased by as much as 75% of their former value. From differential phase the electron concentrations increased by as much as 200%. The changes in electron concentration were greater for differential absorption for altitudes above about 80 kilometers. For differential phase the changes were greater below 80 kilometers.

Fejer (1961) suggested the use of differential absorption and differential phase partial-reflection measurements to calculate collision frequencies. With the information presented above we are able to develop a simple algorithm that will allow us to deduce a collision-frequency profile. This method assumes that given the real collision frequency, the electron concentrations calculated from differential phase and differential absorption are equal. Using the profile of Figure 5.1 as an initial set of collision frequencies the electron concentrations are calculated by both methods. From these electron concentrations a multiplier is calculated as follows:

$$M = N_{DA}/N_{DP}$$

where N_{DA} and N_{DP} are the electron concentration from differential absorption and differential phase respectively. A new value for the collision frequency is found by multiplying the old collision frequency by M. This iterative process is continued until the two calculated electron concentrations are within 0.1 electron cm^{-3} of each other. Approximately six iterations are needed. If this technique is employed for several heights, a set of collision frequencies can be plotted. A least square fit of this set of points gives the new collision-frequency profile.

A collision-frequency profile has been deduced from the data of October 19, 1971 (Figure 5.7). This profile is the dashed line shown in Figure 6.1. The new profile is a least square fit of the collision frequencies plotted nearby. The solid line is the initial profile from Figure 5.1. The new profile is slightly higher and is rotated from the original.

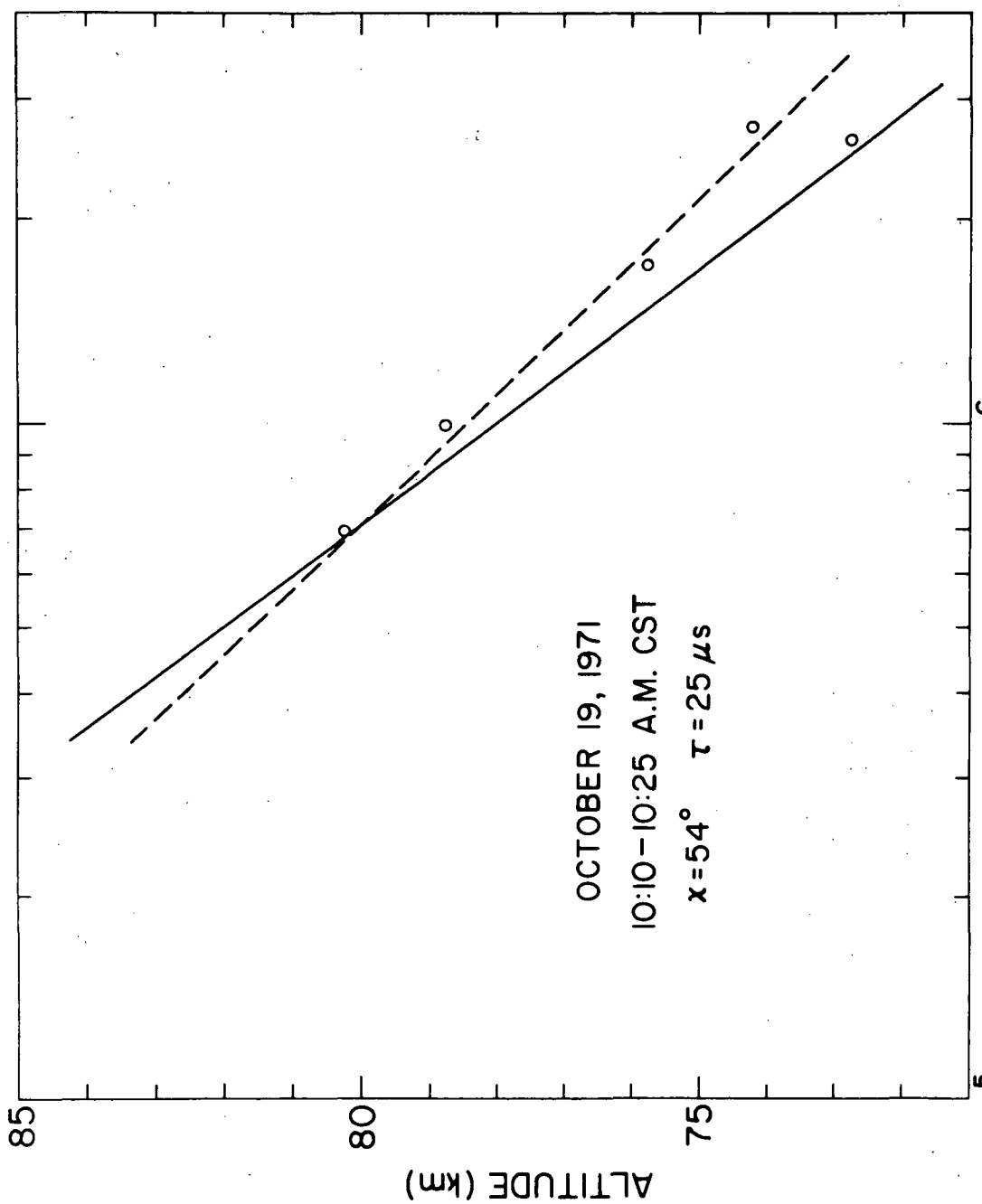

Figure 6.1 Collision frequency profile deduced from differential phase and differential absorption measurements

7. CONCLUSIONS AND SUGGESTIONS FOR FURTHER WORK

A successful demonstration of a differential phase partial-reflection system has been made. Electron-density profiles can be obtained from differential phase measurements over a height range of approximately 75 to 85 kilometers. The Fresnel theory is sufficient to calculate electron concentrations and to evaluate the system. An error analysis is useful for evaluating the system and the results obtained from the system. Differential absorption and differential phase results can be combined to obtain a collision-frequency profile. However, the collision frequency obtained in this manner should be regarded with caution. By comparing the deduced collision-frequency profile with expected profiles, observations as to the validity of the results can be made.

The addition of a differential phase measuring system to the existing partial-reflection experiment would be useful for the study of the lower ionosphere. Differential phase results provide a check on the reliability of the differential absorption results. A partial-reflection system consisting of both differential absorption and differential phase would be useful for studying both D-region ionization and the reflection processes.

Several improvements of the partial-reflection system in general and differential phase measurements in particular are recommended. An improved receiver design would allow more versatility in programming. With a receiver having a linear output, the time required for collecting and processing data would be decreased by more than 50%. The six pulses should be measured sequentially instead of in three segments. The present pulser should be replaced by a digital input-output register that would allow the computer to control the system. The different amplitudes would be obtained by writing the proper software.

Further investigation of the use of volume scattering theory for evaluation of differential phase measurements is recommended. The correlation coefficients from an assumed electron-density profile should be compared with the phase difference calculations. Also, the magnitude of the correlation coefficient should be used in conjunction with the phase difference and A_x/A_o ratio measurements for investigating the performance of the system.

The use of statistical data analysis for evaluating partial-reflection data is recommended. The standard deviations, developed in Chapter 6, give some measure of the confidence that can be placed in the measurement. It would be desirable to incorporate this analysis as a routine part of the data processing.

REFERENCES

Austin, G. L. (1971), A direct measuring differential phase experiment, J. Atmos. Terr. Phys. 33, 1667-1674.

Austin, G. L., R. G. J. Bennett, and M. R. Thorpe (1969), The phase of waves partially reflected from the lower ionosphere (70-120 km), J. Atmos. Terr. Phys. 31, 1099-1106.

Belrose, J. S. (1970), Radio wave probing of the ionosphere by the partial reflection of radio waves (from heights below 100 km), J. Atmos. Terr. Phys. 32, 567-596.

Belrose, J. S. and M. J. Burke (1964), Study of the lower ionosphere using partial reflection I. Experimental technique and method of analysis, J. Geophys. Res. 69, 2799-2818.

Birley, M. H. and C. F. Sechrist, Jr. (1971), Partial reflection data collection and processing using a small computer, Aeronomy Report #42, University of Illinois, Urbana, Illinois.

Booker, H. G. (1959), Radio scattering in the lower ionosphere, J. Geophys. Res. 64, 2164-2177.

Carpenter, L. A. and S. A. Bowhill (1971), Investigation of the physics of dynamical processes in the topside F-region, Aeronomy Report #44, University of Illinois, Urbana, Illinois.

Connolly, D. J. (1971), Differential phase shift of partially reflected radio waves, Radio Sci. 6, 757-762.

Fejer, J. A. (1961), The absorption of short radio waves in the ionosphere D and E regions, J. Atmos. Terr. Phys. 23, 260-274.

Ferraro, A. J. (1959), Experimental and theoretical investigations of the low frequency polarization at 60, 75, and 150 kc/s, Scientific Report No. 121, Ionospheric Research Laboratory, The Pennsylvania State University.

Flood, W. A. (1968), Revised theory for partial reflection D-region measurements, J. Geophys. Res. 73, 5585-5598.

Fraser, G. J. and R. A. Vincent (1970), A study of D-region irregularities, J. Atmos. Terr. Phys. 32, 1591-1607.

Gardner, F. F. and J. L. Pawsey (1953), Study of the ionospheric D-region using partial reflections, J. Atmos. Terr. Phys. 3, 321-344.

Gregory, J. B. and A. H. Manson (1967), Mesospheric electron number densities at 35°S latitude, J. Geophys. Res. 72, 1073-1080.

Gregory, J. B. and R. A. Vincent (1970), Structure of partially reflecting regions in the lower ionosphere, J. Geophys. Res. 75, 6387-6389.

Hara, E. H. (1963), Approximations to the semiconductor integrals $C_p(x)$ and $D_p(x)$ for use with the generalized Appleton-Hartree magneto-ionic formulas, J. Geophys. Res. 68, 4388-4389.

Henry, G. W. (1966), Instrumentation and preliminary results from shipboard measurements of vertical incidence ionospheric absorption, Aeronomy Report #13, University of Illinois, Urbana, Illinois.

Lodato, R. F. and E. A. Mechtly (1971), Rocket measurements of electron collision frequency, Aeronomy Report #45, University of Illinois, Urbana, Illinois.

Mechtly, E. A., S. A. Bowhill, and L. G. Smith (1972), Changes of lower ionosphere electron concentrations with the sunspot cycle, To be published in J. Atmos. Terr. Phys., 1972.

Mechtly, E. A., S. A. Bowhill, L. G. Smith, and H. W. Knoebel (1967), Lower ionosphere electron concentration and collision frequency from rocket measurements of Faraday rotation, differential absorption and probe current, J. Geophys. Res. 72, 5239-5245.

Mechtly, E. A. and L. G. Smith (1968), Seasonal variation of the lower ionosphere at Wallops Island during the IQSY, J. Atmos. Terr. Phys. 30, 1555-1561.

Parkinson, R. W. (1955), Instrumentation for the continuous measurement of certain ionospheric echo characteristics, Rev. of Scient. Instruments 26(4), 319-323.

Pirnat, C. R. and S. A. Bowhill (1966), Electron densities in the lower ionosphere deduced from partial reflection measurements, Aeronomy Report #29, University of Illinois, Urbana, Illinois.

Ratcliffe, J. A. (1959), The Magneto-ionic Theory and Its Applications to the Ionosphere, Cambridge University Press.

Reynolds, D. A. and C. F. Sechrist, Jr. (1970), Measurement of average electron density between 75 and 80 kilometers, Aeronomy Report #36, University of Illinois, Urbana, Illinois.

Sen, H. K. and A. A. Wyller (1960), On the generalization of the Appleton-Hartree magneto-ionic formulas, J. Geophys. Res. 65, 3931-3950.

Thrane, E. V., A. Haug, B. Bjelland, M. Anastassiades, and E. Tsagakis (1968), Measurements of D-region electron densities during the International Quiet Sun Years, J. Atmos. Terr. Phys. 30, 135-150.

Von Biel, H. A. (1971), Determination of D region electron densities within the scattering region, J. Geophys. Res. 76, 5365-5367.

Von Biel, H. A., W. A. Flood, and H. G. Camniz (1970), Differential-phase partial reflection technique for the determination fo D-region ionization, J. Geophys. Res. 75, 4863-4870.

APPENDIX

List of symbols used in the computer programs

Ao = amplitude of ordinary polarized waves

Ax = amplitude of extraordinary polarized waves

A1 = linear polarization corresponding to A_1 in the text

A2 = linear polarization corresponding to A_2 in the text

A3 = linear polarization corresponding to A_3 in the text

A4 = linear polarization corresponding to A_4 in the text

HT = altitude in kilometers

RHD = amplitude of the correlation coefficient

RHOI = imaginary part of the correlation coefficient

RHOR = real part of the correlation coefficient

PHI = $\Delta\phi$

DPHI = $\Delta\phi_2 - \Delta\phi_1$

GNU = ν_m

PL = $\omega + \omega_L$

QL = $\omega - \omega_L$

OMEG = angular operating frequency

CTO = $\mathfrak{C}_{3/2}\left(\frac{\omega + \omega_L}{\nu_m}\right)$

CTX = $\mathfrak{C}_{3/2}\left(\frac{\omega - \omega_L}{\nu_m}\right)$

CFO = $\mathfrak{C}_{3/2}\left(\frac{\omega + \omega_L}{\nu_m}\right)$

CFX = $\mathfrak{C}_{5/2}\left(\frac{\omega - \omega_L}{\nu_m}\right)$

TITLE: DIFASE

```
*       *       *       *       *       *       *       *       *
  PURPOSE: SUBROUTINE TO CALCULATE DIFFERENTIAL PHASE FROM AO,AX,
  A1,A2,A3, AND A4.
  THE PROPER QUADRANT IS FOUND BY EXAMINING THE SIGNS OF THE NUMERATOR
  AND DENOMINATOR BEFORE TAKING THE ARCTANGENT.  THE CHANGE IN
  DIFFERENTIAL PHASE BETWEEN TWO HEIGHTS IS FOUND BY SUBTRACTING
  THE PHASE AT A LOWER HEIGHT FROM THAT AT A HIGHER HEIGHT.  THE
  ANGLES ARE IN DEGREES.
*       *       *       *       *       *       *       *       *
        SUBROUTINE DIFASE(HT,MM,NN,AO,AX,A1,A2,A3,A4,PHI)
        DIMENSION HT(50),AX(50),AO(50),A1(50),A2(50),A3(50),A4(50),
       1RHOR(50),RHOI(50),RHO(50),PHI(50)
        DO 25 J=MM,NN
        CIR=AO(J)**2+AX(J)**2
        BLINR=A1(J)**2+A2(J)**2
        BLINI=A3(J)**2+A4(J)**2
25      WRITE(6,30)HT(J),CIR,BLINR,BLINI
30      FORMAT(5X,F5.2,4X,F10.2,4X,F10.2,4X,F10.2)
        WRITE(6,31)
31      FORMAT(1H1,1X,6HHEIGHT,4X,8HRHO REAL,6X,8HRHO IMAG,9X,3HRHO,
       18X,3HPHI)
        DO 100 K=MM,NN
        PROD=AO(K)*AX(K)
        RNUM=(A1(K)**2-A2(K)**2)*(AO(K)**2+AX(K)**2)
        RDEN=(A1(K)**2+A1(K)**2)*PROD
        RHOR(K)=RNUM/(2.0*RDEN)
        GNUM=(A4(K)**2-A3(K)**2)*(AO(K)**2+AX(K)**2)
        GDEN=(A4(K)**2+A3(K)**2)*PROD
        RHOI(K)=GNUM/(2.0*GDEN)
        ARHOI=ABS(RHOI(K))
        ARHOR=ABS(RHOR(K))
        IF(RHOI(K).LT.0.0)GO TO 40
        IF(RHOR(K).LT.0.0)GO TO 35
        PHI(K)=57.29578*ATAN(ARHOI/ARHOR)
        GO TO 50
35      PHI(K)=180.0-57.29578*ATAN(ARHOI/ARHOR)
        GO TO 50
40      IF(RHOR(K).LT.0.0)GO TO 45
        PHI(K)=360.0-57.29578*ATAN(ARHOI/ARHOR)
        GO TO 50
45      PHI(K)=180.0+57.29578*ATAN(ARHOI/ARHOR)
50      CONTINUE
        RHO(K)=SQRT(RHOI(K)**2+RHOR(K)**2)
100     WRITE(6,75)HT(K),RHOR(K),RHOI(K),RHO(K),PHI(K)
75      FORMAT(2X,F5.2,2X,E12.8,2X,E12.8,2X,E12.8,2X,F10.4)
        RETURN
        END
```

```
                        TITLE: PROAXD
*       *       *       *       *       *       *       *       *       *
  PURPOSE: SUBROUTINE TO READ DATA FROM DECTAPE, AVERAGE IT, AND
  CALCULATE ELECTRON CONCENTRATIONS.
  SUBROUTINES CALLED: DREAD,CALC
  THE DATA FROM THE DECTAPE ARE SQUARED AND AVERAGED.  THE MEAN
  SQUARED NOISE OF EACH POLARIZATION IS SUBTRACTED FROM THE MEAN
  SQUARED AMPLITUDE.  THE RMS AVERAGES FOR THE NOISE AND THE AMPLI-
  TUDES ARE TABULATED FOR EACH ALTITUDE.  ELECTRON CONCENTRATIONS
  FOR AX AND AO DATA ONLY ARE CALCULATED BY SUBROUTINE CALC.  DREAD
  AND CALC ARE SUBROUTINES USED IN THE AERONOMY LAB FOR DIFFERENTIAL
  ABSORPTION WORK.
*       *       *       *       *       *       *       *       *       *
        SUBROUTINE PROAXD(FNAM,M,BMXNS,RE1,RE2,HT,AVAO,AVAX)
        DIMENSION FNAM(2),AA(21),AB(21),AVAO(21),AVAX(21),
       1XO(21),IRJO(21),IRJX(21),DIFNO(4),DIFNX(4),HT(21),
       2BO(21),BX(21),BNO(4),BNX(4),BNXN(4),AXN(21),BBNO(4),BBNX(4)
        SNO=0.
        SNX=0.
        IR=0
        IRNO=0
        IRNX=0
        BMO=0.
        BMX=0.
        DO 16 I=1,21
        XO(I)=0.
        AVAO(I)=0.
        AVAX(I)=0.
        AA(I)=0.
        AB(I)=0.
        IRJO(I)=0
16      IRJX(I)=0
        DO 17 I=1,4
        BNO(I)=0.
17      BNX(I)=0.
        CALL VALUE
        CALL DINIT
        CALL FSTAT(2,FNAM,LOG)
        IF(LOG.NE.0)GO TO 40
        WRITE(6,35)FNAM
35      FORMAT(6H FILE ,2A5,19H NOT FOUND ON DAT 2)
        RETURN
40      CALL SEEK(2,FNAM)
        KEOFO=0
        KEOFX=0
        ID=0
48      DO 148 I=1,21
        BO(I)=AA(I)
148     BX(I)=AB(I)
        DO 149 I=1,4
        BBNO(I)=BNO(I)
```

```
149     BBNX(I)=BNX(I)
        CALL DREAD(AA,BNO,IERR,ID,KEOFO)
        IF(KEOFO.EQ.1)GO TO 50
        CALL DREAD(AB,BNX,IERR,ID,KEOFX)
        IF(KEOFX.EQ.1)GO TO 49
201     BMEANO=0.
        BMEANX=0.
        DO 440 I=1,4
        BMEANO=BMEANO+BNO(I)**2
440     BMEANX=BMEANX+BNX(I)**2
        BMEANO=SQRT(BMEANO/4.)
        BMEANX=SQRT(BMEANX/4.)
        IF(BMEANO.GT.BMXNS.AND.BMEANX.GT.BMXNS)GO TO 510
        DO 220 I=1,4
        DIFNO(I)=BNO(I)-BBNO(I)
220     DIFNX(I)=BNX(I)-BBNX(I)
        DO 221 I=1,2
        J=I+1
        K=I+2
        IF(DIFNO(I).GT.RE1.OR.DIFNO(J).GT.RE1.OR.DIFNO(K).GT.RE1.OR.
       1BNO(J).GT.510..OR.BNX(J).GT.510.)GO TO 710
        BMO=BMO+BNO(J)**2
        GO TO 715
710     IRNO=IRNO+1
        IF(BNO(J).GT.510..OR.BNX(J).GT.510.)GO TO 720
715     IF(DIFNX(I).GT.RE1.OR.DIFNX(J).GT.RE1.OR.DIFNX(K).GT.RE1)
       1 GO TO 720
        BMX=BMX+BNX(J)**2
        GO TO 221
720     IRNX=IRNX+1
221     CONTINUE
730     DO 47 I=1,21
        J=I+1
        L=I-1
        IF(L.EQ.0)L=1
        IF(J.GT.21)J=21
        DIFE=AA(I)-BO(I)
        DIFEA=AA(L)-BO(L)
        DIFEB=AA(J)-BO(J)
        IF(I.GT.9)GO TO 301
        IF(DIFE.GT.RE1.OR.DIFEA.GT.RE1.OR.DIFEB.GT.RE1.OR.
       1AA(I).GT.510..OR.AB(I).GT.510.)GO TO 45
        GO TO 110
301     IF(DIFE.GT.RE2.OR.DIFEA.GT.RE2.OR.DIFEB.GT.RE2.OR.
       1AA(I).GT.510..OR.AB(I).GT.510.)GO TO 45
110     AVAO(I)=AVAO(I)+AA(I)**2
        GO TO 111
45      IRJO(I)=IRJO(I)+1
        IF(AA(I).GT.510..OR.AB(I).GT.510.)GO TO 46
111     DIFE=AB(I)-BX(I)
        DIFEA=AB(L)-BX(L)
        DIFEB=AB(J)-BX(J)
```

```
      IF(I.GT.9.AND.I.LT.16)GO TO 303
      IF(DIFE.GT.RE1.OR.DIFEA.GT.RE1.OR.DIFEB.GT.RE1)GO TO 46
      GO TO 120
303   IF(DIFE.GT.RE2.OR.DIFEA.GT.RE2.OR.DIFEB.GT.RE2)GO TO 46
120   AVAX(I)=AVAX(I)+AB(I)**2
      GO TO 47
46    IRJX(I)=IRJX(I)+1
47    CONTINUE
      GO TO 520
510   IR=IR+1
520   SNO=BMEANO**2+SNO
      SNX=BMEANX**2+SNX
      GO TO 48
49    ID=ID-1
50    ID=ID/2
      BID=ID
      DO 830 I=1,21
      IRJO(I)=IRJO(I)+IR
830   IRJX(I)=IRJX(I)+IR
      IRNO=IRNO+2*IR
      IRNX=IRNX+2*IR
      AVNO=SQRT(SNO/BID)
      AVNX=SQRT(SNX/BID)
      RNO=ID*2-IRNO
      RNX=ID*2-IRNX
      DO 52 I=1,21
      RSAMO=ID-IRJO(I)
      RSAMX=ID-IRJX(I)
      AVOC=AVAO(I)/RSAMO-BMO/RNO
      AVXC=AVAX(I)/RSAMX-BMX/RNX
      AVAO(I)=(ABS(AVOC)/AVOC)*SQRT(ABS(AVOC))
      AVAX(I)=(ABS(AVXC)/AVXC)*SQRT(ABS(AVXC))
52    CONTINUE
      BMO=SQRT(BMO/RNO)
      BMX=SQRT(BMX/RNX)
      CALL HEAD(1)
      WRITE(6,153)AVNO,AVNX,BMO,IRNO,BMX,IRNX
153   FORMAT(2X,17HAVERAGE NOISE ORD,F8.1/2X,17HAVERAGE NOISE EXT,1X
     1,F7.1//2X,9HNOISE ORD,F8.1,I5,11H REJECTIONS/2X,
     29HNOISE EXT,F8.1,I5,11H REJECTIONS)
      WRITE(6,54)ID,IR
54    FORMAT(//1X,I4,14H SAMPLES TAKEN,5X,I5,16H FRAMES REJECTED//
     19H REJECTED,2X,9H REJECTED,2X,6HHEIGHT,2X,6HAV. AO,2X,
     26HAV. AX/4X,3HOPD,8X,3HEXT)
      HTIN=58.5
      DO 53 I=1,21
      XZ=I
      HT(I)=HTIN+XZ*1.5
      WRITE(6,58)IRJO(I),IRJX(I),HT(I),AVAO(I),AVAX(I)
58    FORMAT(3X,I4,7X,I4,3X,F5.1,3X,F6.1,2X,F6.1)
53    CONTINUE
      IF(M.EQ.2)GO TO 62
```

```
      DO 59 I=1,21
      IF(AVA0(I).LE.0.0.OR.AVAX(I).LE.0.0)GO TO 59
      X0(I)=AVAX(I)/AVA0(I)
59    CONTINUE
      CALL CALC(X0,1,20,RESP)
62    RETURN
      END
```

```
                        TITLE: MASTER
*       *       *       *       *       *       *       *
  PURPOSE: DATA PROCESSING CONTROL PROGRAM
  SUBROUTINES CALLED: PROAXD,DIFASE
  PROCESSING INFORMATION SUCH AS THE DATAFILE AND NOISE CRITERIA
  IS READ INTO THE PROGRAM. PROAXD IS CALLED 3 TIMES.  THE FIRST
  TIME AX AND A0 DATA ARE PROCESSED AND AN ELECTRON CONCENTRATION
  PROFILE IS CALCULATED.  THE SECOND TIME A1 AND A2 DATA ARE PRO-
  CESSED, TABULATED, AND STORED IN AN ARRAY.  THE THIRD TIME
  A3 AND A4 DATA ARE PROCESSED, TABULATED, AND STORED IN AN ARRAY.
  DIFASE IS THEN CALLED TO CALCULATE DIFFERENTIAL PHASE FROM A0,
  AX,A1,A2,A3, AND A4.
*       *       *       *       *       *       *       *
      DIMENSION FNAM(2),AA(21),AB(21),AVA0(21),AVAX(21),
     1X0(21),IRJ0(21),IRJX(21),DIFN0(4),DIFNX(4),B0(21),BX(21),
     2BN0(4),BNX(4),BNXN(4),AXN(21),BBN0(4),BBNX(4),A0(21),
     3AX(21),A1(21),A2(21),A3(21),A4(21),HT(21),RHOR(21),RHOI(21),
     4RHO(21),PHI(21),DPHI(21)
5     CALL HEAD(0)
      WRITE(6,10)
10    FORMAT(15H WHICH DATAFILE)
      READ(4,20)FNAM
20    FORMAT(2A5)
      M=1
      WRITE(6,25)
25    FORMAT(24H COLLISION FREQ. PROFILE/
     1 25H SUMMER,WINTER,OR EQUINOX)
      READ(4,30)RESP
30    FORMAT(A5)
      WRITE(6,35)
35    FORMAT(14H MAXIMUM NOISE)
      READ(4,40)RMXNS
40    FORMAT(F10.0)
      WRITE(6,45)
45    FORMAT(21H REJECTION BELOW 72KM)
      READ(4,40)RE1
      WRITE(6,50)
50    FORMAT(21H REJECTION ABOVE 72KM)
      READ(4,40)RE2
      CALL PROAXD(FNAM,M,RMXNS,RE1,RE2,HT,A0,AX)
      M=2
      WRITE(6,10)
      READ(4,20)FNAM
```

```
      CALL PROAXD(FNAM,M,RMXNS,RE1,RE2,HT,A1,A2)
      WRITE(6,10)
      READ(4,20)FNAM
      CALL PROAXD(FNAM,M,RMXNS,RE1,RE2,HT,A3,A4)
      WRITE(6,55)
55    FORMAT(15H INITIAL HEIGHT)
      READ(4,40)HT1
      WRITE(6,60)
60    FORMAT(13H FINAL HEIGHT)
      READ(4,40)HT2
      MM=(HT1-58.5)/1.5
      NN=(HT2-58.5)/1.5
      CALL DIFASE(HT,MM,NN,A0,AX,A1,A2,A3,A4,PHI)
      WRITE(6,65)
65    FORMAT(///7H HEIGHT,2X,16HPHASE DIFFERENCE)
      L=NN-1
      DO 70 LM=MM,L
      MK=LM+1
      DPHI(LM)=PHI(MK)-PHI(LM)
      HTD=HT(LM)+0.75
70    WRITE(6,75)HTD,DPHI(LM)
75    FORMAT(2X,F5.2,4X,F10.4)
      GO TO 5
      END
```

```
C                        TITLE: PHELD
C       *       *       *       *       *       *       *       *
C PURPOSE: CALCULATE ELECTRON CONCENTRATIONS FROM PHASE DATA
C AN ASSUMED COLLISION FREQUENCY PROFILE IS STORED IN MEMORY.  THE
C PHASE DIFFERENCE IS READ IN SEQUENTIALLY FROM THE LOWEST HEIGHT.
C THE QUASI-LONGITUDINAL APPROXIMATION TO THE GENERALIZED FORMULA
C FOR THE REFRACTIVE INDEX IS USED.  THE FRESNEL MODEL WAS USED TO
C CALCULATE REFLECTION COEFFICIENTS.  THE ELECTRON CONCENTRATION IS
C PRINTED OUT IN ELECTRONS PER CUBIC CENTIMETER.
C       *       *       *       *       *       *       *       *
      DIMENSION DPHI(20),GNU(21),EN(20)
      C3(X)=(X*(X*(X*(X+24.653115)+113.9416)+11.287513)+.023983474)
     1/(X*(X*(X*(X*(X*(X+24.656819)+120.49512)+289.58085)+149.21254)
     2+9.3872372)+.018064128)
      C5(X)=(X*(X*(X+6.6945939)+16.901002)+1.1630641)/(X*(X*(X*(X*(X+
     16.6314497)+35.355257)+68.920505)+64.093464)+4.3605732)
C ENTER COLLISION FREQUENCY PROFILE
      GNU(1)=2.20E7
      GNU(2)=1.72E7
      GNU(3)=1.32E7
      GNU(4)=1.04E7
      GNU(5)=8.0E6
      GNU(6)=6.2E6
```

```
      GNU(7)=4.8E6
      GNU(8)=3.7E6
      GNU(9)=2.85E6
      GNU(10)=2.2E6
      GNU(11)=1.70E6
      GNU(12)=1.3E6
      GNU(13)=1.0E6
      GNU(14)=7.8E5
      GNU(15)=6.0E5
      GNU(16)=4.6E5
      GNU(17)=3.6E5
      GNU(18)=2.75E5
      GNU(19)=2.12E5
      GNU(20)=1.65E5
      GNU(21)=1.35E5
C ENTER CONSTANTS
      PL=2.59614E+7
      QL=7.3886E+6
      E=1.60210E-19
      EM=9.10908E-31
      PERM=8.854E-12
      OMEG=2.0*3.14159*2.66E+6
10    WRITE(6,100)
100   FORMAT(1H1,15H INITIAL HEIGHT)
      READ(4,110)HT1
110   FORMAT(F10.0)
      WRITE(6,120)
120   FORMAT(13H FINAL HEIGHT)
      READ(4,110)HT2
      M=(HT1-58.5)/1.5
      N=(HT2-58.5)/1.5
      T=M-1
      HT=59.25+T*1.5
      DO 20 L=M,N
20    READ(4,25)DPHI(L)
25    FORMAT(F10.6)
      WRITE(6,35)
35    FORMAT(1H1)
      WRITE(6,40)
40    FORMAT(7H HEIGHT,4X,9HPHASE DIF,5X,9HCOLL FREQ,4X,9HELEC CONC)
      DO 50 J=M,N
      HT=HT+1.5
C SEN-WYLLER EQUATIONS
      GNU1=(GNU(J)+GNU(J+1))/2.0
      O1=PL/GNU(J)
      O2=PL/GNU(J+1)
      O=PL/GNU1
      X1=QL/GNU(J)
      X2=QL/GNU(J+1)
      X=QL/GNU1
```

```
C REFLECTION COEFFICIENTS
      AMO1=(2.5*C5(O1))/(O1*C3(O1))
      GAMO1=ATAN(AMO1)
      AMX1=(2.5*C5(X1))/(X1*C3(X1))
      GAMX1=ATAN(AMX1)
      AMO2=(2.5*C5(O2))/(O2*C3(O2))
      GAMO2=ATAN(AMO2)
      AMX2=(2.5*C5(X2))/(X2*C3(X2))
      GAMX2=ATAN(AMX2)
      DIFGM1=57.2958*(GAMX1-GAMO1)
      DIFGM2=57.2958*(GAMX2-GAMO2)
      CON=(EM*PERM*3.0E8)/(E*E*1.5E3*57.2958)
C CALCULATE ELECTRON CONCENTRATION
      SUB=QL*C3(X)-PL*C3(O)
      GNU2=GNU1**2
      DELTA=DPHI(J)-DIFGM2+DIFGM1
      ENUM=CON*DELTA*GNU2
      EN(J)=ENUM/SUB
      EN(J)=EN(J)/1.0E6
50    WRITE(6,60)HT,DPHI(J),GNU1,EN(J)
60    FORMAT(2X,F5.2,2X,F10.4,5X,E10.4,2X,F12.6)
      GO TO 10
      END
```